



Calhoun: The NPS Institutional Archive

Theses and Dissertations

Thesis Collection

1984

CSMP modelling of brushless DC motors.

Thomas, Steven M.

<http://hdl.handle.net/10945/19222>



Calhoun is a project of the Dudley Knox Library at NPS, furthering the precepts and goals of open government and government transparency. All information contained herein has been approved for release by the NPS Public Affairs Officer.

Dudley Knox Library / Naval Postgraduate School
411 Dyer Road / 1 University Circle
Monterey, California USA 93943

<http://www.nps.edu/library>

DUDLEY KNOX LIBRARY
MILITARY POSTGRADUATE SCHOOL
MILITARY CALIFORNIA 93943-5002

NAVAL POSTGRADUATE SCHOOL

Monterey, California



THESIS

CSMP MODELLING OF
BRUSHLESS DC MOTORS

by

Steven M. Thomas

September 1984

Thesis Advisor:

A. Gerba

Approved for public release, distribution unlimited

T222463

REPORT DOCUMENTATION PAGE		READ INSTRUCTIONS BEFORE COMPLETING FORM
1. REPORT NUMBER	2. GOVT ACCESSION NO.	3. RECIPIENT'S CATALOG NUMBER
4. TITLE (and Subtitle) CSMP Modelling of Brushless DC Motors		5. TYPE OF REPORT & PERIOD COVERED Master's Thesis; September 1984
		6. PERFORMING ORG. REPORT NUMBER
7. AUTHOR(s) Steven M. Thomas		8. CONTRACT OR GRANT NUMBER(s)
9. PERFORMING ORGANIZATION NAME AND ADDRESS Naval Postgraduate School Monterey, California 93943		10. PROGRAM ELEMENT, PROJECT, TASK AREA & WORK UNIT NUMBERS
11. CONTROLLING OFFICE NAME AND ADDRESS Naval Postgraduate School Monterey, California 93943		12. REPORT DATE September 1984
		13. NUMBER OF PAGES 88
14. MONITORING AGENCY NAME & ADDRESS (if different from Controlling Office)		15. SECURITY CLASS. (of this report) UNCLASSIFIED
		15a. DECLASSIFICATION/DOWNGRADING SCHEDULE
16. DISTRIBUTION STATEMENT (of this Report) Approved for public release, distribution unlimited		
17. DISTRIBUTION STATEMENT (of the abstract entered in Block 20, if different from Report)		
18. SUPPLEMENTARY NOTES		
19. KEY WORDS (Continue on reverse side if necessary and identify by block number) Brushless DC Motors		
20. ABSTRACT (Continue on reverse side if necessary and identify by block number) Recent improvements in rare earth magnets have made it possible to construct strong, lightweight, high horsepower DC motors. This has occasioned a reassessment of electromechanical actuators as alternatives to comparable pneumatic and hydraulic systems for use in flight control actuators for tactical missiles. This thesis develops a low-order mathematical model for the simulation and analysis of brushless DC motor performance. This model is implemented in CSMP language. It is used to predict such motor		

performance curves as speed, current and power versus torque. Electronic commutation based on Hall effect sensor positional feedback is simulated. Steady state motor behavior is studies under both constant and variable air gap flux conditions. The variable flux takes two different forms. In the first case, the flux is varied as a simple sinusoid. In the second case, the flux is varied as the sum of a sinusoid and one of its harmonics.

Approved for public release; distribution unlimited.

CSMP Modelling of
Brushless DC Motors

by

Steven M. Thomas
Lieutenant, United States Navy
B.A., University of Delaware, 1976

Submitted in partial fulfillment of the
requirements for the degree of

MASTER OF SCIENCE IN ELECTRICAL ENGINEERING

from the

NAVAL POSTGRADUATE SCHOOL
September 1984

ABSTRACT

Recent improvements in rare earth magnets have made it possible to construct strong, lightweight, high horsepower DC motors. This has occasioned a reassessment of electromechanical actuators as alternatives to comparable pneumatic and hydraulic systems for use in flight control actuators for tactical missiles. This thesis develops a low-order mathematical model for the simulation and analysis of brushless DC motor performance. The model is implemented in CSMP language. It is used to predict such motor performance curves as speed, current and power versus torque. Electronic commutation based on Hall effect sensor positional feedback is simulated. Steady state motor behavior is studied under both constant and variable air gap flux conditions. The variable flux takes two different forms. In the first case, the flux is varied as a simple sinusoid. In the second case, the flux is varied as the sum of a sinusoid and one of its harmonics.

TABLE OF CONTENTS

I.	INTRODUCTION	9
II.	NATURE OF THE PROBLEM	12
	A. PROGRAMMING LANGUAGE	12
	B. SYSTEM BLOCK DIAGRAM	12
	C. DEVELOPMENT OF MOTOR SYSTEM EQUATIONS	13
III.	CURVE PREDICTION	19
	A. OVERVIEW	19
	B. SPEED VS TORQUE CURVE	20
	C. CURRENT VS TORQUE CURVE	22
	D. OUTPUT POWER VS TORQUE CURVE	22
	E. MOTOR REVERSAL	27
IV.	ELECTRONIC COMMUTATION	28
	A. SWITCHING ACTION	28
	B. HALL EFFECT SENSOR FEEDBACK	30
	C. MODEL REVISION	35
V.	VARIABLE FLUX	36
	A. AIR GAP FLUX	36
	B. FLUX AS AN AVERAGE VALUE	37
	C. SINUSOIDAL FLUX	38
	D. HARMONIC FLUX	41
VI.	SUMMARY	47
	A. REMARKS AND CONCLUSIONS	47
	B. RECOMMENDATIONS FOR FUTURE STUDY	48
APPENDIX A: LISTING OF MODEL PROGRAMS		49
	A. BASIC PROTOTYPE MODEL	49

B. REVISION ONE	52
C. REVISION TWO	58
D. REVISION THREE	63
E. REVISION FOUR	69
APPENDIX B: SAMPLE OUTPUT	75
LIST OF REFERENCES	86
BIBLIOGRAPHY	87
INITIAL DISTRIBUTION LIST	88

LIST OF TABLES

I.	Typical Commercial Motor Parameters	19
II.	Sensor and Switching Logic	32
III.	Torque and Speed Ripple Due to Sinusoidal Flux . .	41
IV.	Torque and Speed Ripple Due to Harmonic Flux . . .	44

LIST OF FIGURES

2.1	Equivalent DC Motor Circuit	14
2.2	Block Diagram of DC Motor	18
3.1	Motor Speed vs Torque Curve	23
3.2	Family of Speed-Torque Curves	24
3.3	Motor Current vs Torque Curve	25
3.4	Output Power vs Torque Curve	26
4.1	Controller Configuration	28
4.2	Switching Logic of a 3-Phase Brushless DC Motor	29
4.3	Equivalent Circuit With Electronic Commutation.	31
4.4	The Hall Effect	33
4.5	Sensor Logic Based on a Hall Effect Sensor . . .	34
5.1	Composite Flux Variation for Two Windings . . .	39
5.2	Back EMF Waveform Due to Harmonic Flux	43

I. INTRODUCTION

Direct current electric motors are gaining wider use in space applications where long life, high reliability, high torque and light weight are critical factors. In recent years, advances in magnet technology and materials, especially the use of rare earth magnets, have made possible significant improvements in the torque to inertia ratios of permanent magnet (PM) motors. Samarium cobalt is one such rare earth magnetic material. The great potential of the rare earth magnets derive from their inherent high flux density and high coercivity properties. Higher flux densities mean greater developed motor torque while high coercivity means greater innate resistance to demagnetization which permits thinner magnet sections. The two factors in combination result in increased mechanical power and energy product with decreased physical size and weight.

Brushless dc motors belong to this class of permanent magnet motors and thus enjoy their improved torque to size characteristics. In fact, brushless dc motors are significantly smaller than either their ac counterparts or conventional brush-type dc motors on an equal horsepower basis. Compared to its conventional counterpart, a brushless dc motor's structure is "inside out." In the brushless configuration, the permanent magnets are attached to the rotor and the conducting coils are placed in the stator. As its name suggests, brushes have been eliminated from this type of motor. Instead, commutation of current in the stationary armature is accomplished electronically by switching on the appropriate windings via transistors specially designed to provide the high currents needed for motor power. In order to sequence the current to the coils, the commutation circuitry is provided rotor position feedback from sensing

devices, most commonly from Hall effect sensors. These are simple semiconductor devices that develop a polarized voltage depending upon the magnetic field passing through them. Small, highly sensitive and reliable, Hall effect sensors require little power to operate and thus are widely used.

Brushless dc motors possess all the advantages traditionally associated with conventional dc motors such as linear torque-speed characteristics, excellent response times and high efficiency. In addition, there are a number of important advantages that brushless dc motors possess over standard brush-type dc motors. An obvious advantage is that electronic commutation means the elimination of commutators, the wear and tear of brushes, and the build up of carbon dust which heretofore significantly limited the life of the standard dc motor. Since electronic current switching essentially involves no component wear, there results improved reliability and enhanced lifespan. As well as being subject to wear and tear, the action of brushes sliding over commutators also generates radio frequency interference (RFI) which is a severe liability in many applications. In fact, it is often in hostile and explosive environments that the advantages of dc motors are most needed. Another benefit is in heat transfer characteristics. By placing windings in the stator the thermal path to the environment is made shorter and more direct. With the removal of heat thus enhanced, mechanical and electrical malfunctions due to heat are reduced. A further important advantage of the brushless dc motor is in the area of motor speed variability. Whereas ac motors usually operate at one speed fixed by the powerline frequency, any dc motor's speed can be changed to meet varying power requirements by simply adjusting the dc input voltage. The electronic commutation scheme of the brushless dc motor lends itself nicely to just

this type of variable speed control. It is a relatively simple matter to attach to the commutation circuit board a small, inexpensive microprocessor whose logic can be programmed to run the motor at any of several speeds or in either direction. A single motor can thus be programmed, in place if desired, so that its speed, direction and torque are matched to a particular application.

There are at least as many applications for brushless dc motors as there are for brush-type motor systems as well as a host of new applications. Of particular relevance to this thesis is the use of brushless dc motors in flight control actuator systems of Navy tactical missiles, in particular, the cruise missile. There are three general types of actuators that are in use in missile systems: pneumatic, hydraulic and electromechanical. The maneuvering requirements of the more advanced tactical missiles call for high control torques which heretofore could only be produced by high pressure pneumatic or hydraulic actuators. Both of these actuator systems are more susceptible to mechanical malfunction than their electrical counterparts. With the improved torque to inertia ratios resulting from better rare earth magnet materials and the higher mechanical reliability due to removal of brushes, as well as other advantages previously enumerated, the brushless dc motor is in a position to compete with most pneumatic and hydraulic systems. This thesis is but one part of a detailed study of the state of the art in electromechanical actuators as applied to the cruise missile system [Ref. 1].

II. NATURE OF THE PROBLEM

A. PROGRAMMING LANGUAGE

The objective of this thesis is to create a simplified low-order mathematical model that will accurately simulate the response of a brushless dc motor. The IBM Continuous System Modeling Program (CSMP) was chosen for use since it is a user-oriented computer language specifically created for modeling dynamic physical systems and is one of the most widely used in this area [Ref. 2]. It has the flexibility of determining the response of a system that is modeled either in a block diagram format or as a set of ordinary differential equations. While CSMP is an offshoot of IBM's Digital Simulation Language, it embodies Fortran as its source language and retains much of Fortran's capability and flexibility. CSMP is an applications-oriented program intended for use with the IBM mainframe systems. The utility and ease of using this program language stems from simplified program control statements that almost exactly describe the mathematical equations or physical variables of the system and from the flexibility of its program structure which contains preprogrammed function blocks that obviate the need for complicated subroutine programming. In essence, CSMP was chosen because it permits the user to concentrate on the details of the physical system rather than on the time-consuming complexities of programming.

B. SYSTEM BLOCK DIAGRAM

The block diagram format was chosen as the basis for the CSMP program since it is a convenient way of analyzing the input-output relationships of a physical system and the

flow of signals through it without having to refer to the system equations. The basic idea of a block diagram stems from the application of Laplace transforms to a system's integro-differential or differential equations. In effect, a differential equation is rendered into a simpler algebraic expression which, in turn, becomes a fundamental equation of a system's functional blocks. Each block indicates the relationship between its input driving signal and output response; ie., the transfer function of the input and output. The transfer function is defined as the ratio of the Laplace transform of the output to the transform of the input with all initial conditions assumed to be zero. A block's transfer function does not include any information about the internal structure of that part of a system, merely the transformation of a signal between two points in a system. Furthermore, it should be borne in mind that all physical systems have certain transfer characteristics that are actually nonlinear to some extent. A dc motor system can be fairly accurately described using the transfer function approach to modeling and, when nonlinear transfer characteristics exist, CSMP modeling can usually be obtained from preprogrammed nonlinear function routines.

C. DEVELOPMENT OF MOTOR SYSTEM EQUATIONS

In order to construct the block diagram of a system, one approach is to identify the various mathematical relationships between the components of the system and to write balance equations that will identify each individual block comprising the system. The system equations for a brushless dc motor are presented in chapter three where all the details of the logic control and switching of transistors for commutation of the motor are developed. What follows is a simplified input-output characteristics model of the type

that has been a standard for brush-type dc motors used in control system studies [Ref. 3]. The development of this input-output model is the first learning step in the modeling process for the brushless dc motor and has the additional usefulness of being a tool for a concurrent mechanical engineering study of load torque requirements for the motor [Ref. 1].

To write the electrical balance equation describing a basic dc motor, the classical loop method based on Kirchoff's voltage law is applied to the equivalent motor circuit (Figure 2.1).

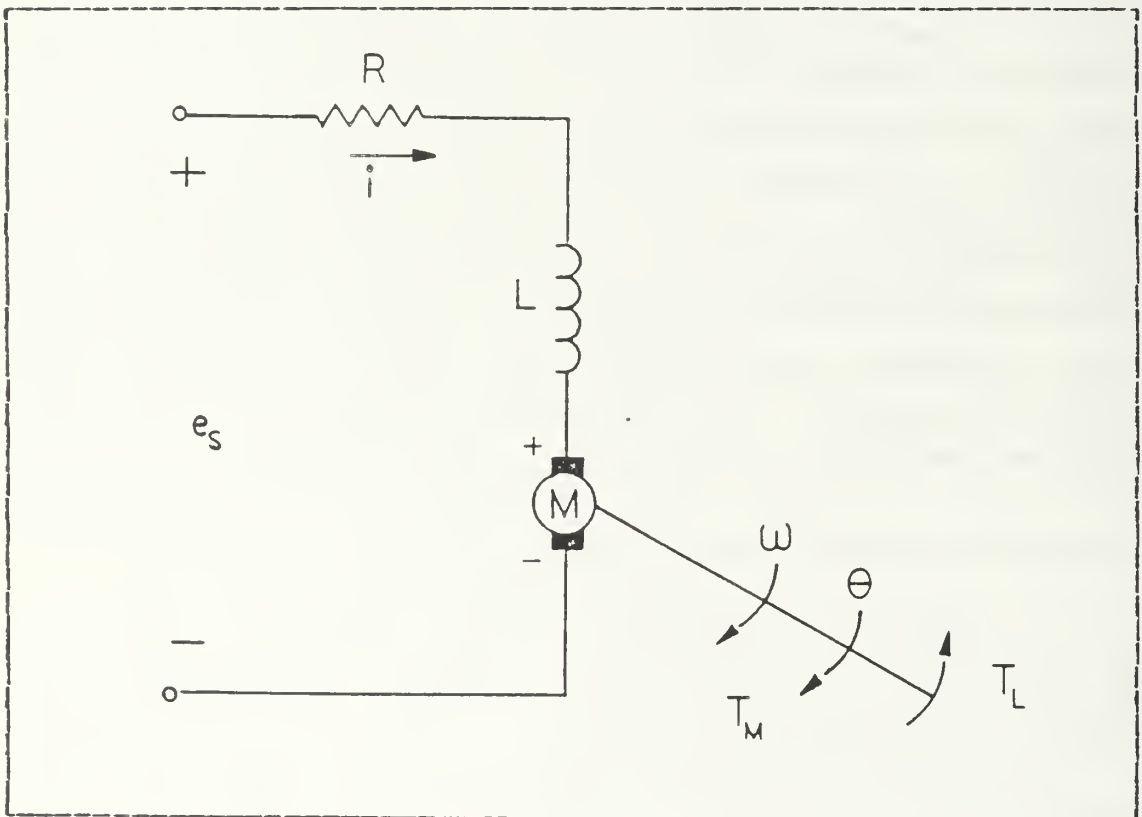


Figure 2.1 Equivalent DC Motor Circuit

The basic dc motor has the coil windings on the armature and the magnetic field source on the stator. In the case of the brushless dc motor, the rotor consists of permanent magnets that produce the magnetic field and the stator contains the coil windings. The Kirchoff Law for the stator circuit is

$$e_s(t) = L di/dt + R i(t) + e_b(t) \quad (\text{eqn 2.1})$$

where R and L are the stator resistance and inductance respectively, and $e_b(t)$ is the back emf. When a conductor moves in a magnetic field, or there is any relative motion between the magnetic field source and the conductor, a voltage is generated across the terminals of the conductor. In the case of the dc motor, the voltage is proportional to the shaft velocity and tends to oppose the current flow. The relationship between the back emf and the shaft velocity is

$$e_s(t) = (K_m \phi) \omega_m(t) = K_b \omega_m(t) \quad (\text{eqn 2.2})$$

$$e_s(t) = K_b d\theta_m(t)/dt \quad (\text{eqn 2.3})$$

Substituting and rearranging equations 2.1 and 2.2 into their differential forms gives the following two equations.

$$di/dt = (1/L) e_s(t) - (R/L) i(t) - (1/L) K_b \omega_m(t) \quad (\text{eqn 2.4})$$

$$d\theta_m(t)/dt = \omega_m(t) \quad (\text{eqn 2.5})$$

The basic balance equation that describes the motor as a mechanical system derives from application of Newton's laws of motion to the system components. The dynamic equation for a motor coupled to its load is

$$t_m(t) = J d\omega_m(t)/dt + B \omega_m(t) + t_l(t) \quad (\text{eqn 2.6})$$

where $t_l(t)$ is the load torque. Rearranging the equation it becomes

$$d\omega_m(t)/dt = (1/J) * t_m(t) - (1/J) * t_l(t) - (B/J) * \omega_m(t) \quad (\text{eqn 2.7})$$

B is the total viscous friction coefficient of the motor and is comprised of the sum of the viscous friction due to the motor, B_m , and the load, B_l , as seen by the motor shaft. Likewise, J is the total system inertia comprised of the sum of the motor inertia, J_m , and of the load inertia, J_l , reflected through the coupling device to the motor shaft. Both B_l and J_l are functions of the motor's speed reducing mechanism where N is the speed reduction ratio ($N > 1$). The following equations summarize the foregoing.

$$B = B_m + B_l \quad (\text{eqn 2.8})$$

$$J = J_m + J_l \quad (\text{eqn 2.9})$$

$$B_l = B_{lp}/N \quad (\text{eqn 2.10})$$

$$J_l = J_{lp}/N \quad (\text{eqn 2.11})$$

J_{lp} and B_{lp} are the inertia and viscous friction seen at the load side of the system. Since a dc motor is essentially a torque transducer that converts electrical energy into mechanical energy, the following equation is necessary to show the relationship among the developed torque, $t_m(t)$, the air gap flux, ϕ , and the stator current, $i(t)$.

$$t_m(t) = (K_m * \phi) * i(t) \quad (\text{eqn 2.12})$$

Because the magnetic field in the motor is assumed uniform and constant, this can be simplified to

$$t_m(t) = K_t i(t) \quad (\text{eqn 2.13})$$

where K_t is the torque constant of the motor.

Equations 2.1 through 2.13 represent the cause and effect equations of the system. The application of $e_s(t)$ produces a current flow which causes the torque and the back emf to be generated. The torque produced then causes the angular displacement $\theta_m(t)$. Given the differential equations of the system, the Laplace transform can be applied and the block diagram of the system generated. As an example, the block for equation 2.1 is generated as follows

$$e_s(t) - e_b(t) = L di/dt + R i(t) \quad (\text{eqn 2.14})$$

$$\mathcal{L}\{e_s(t) - e_b(t)\} = \mathcal{L}\{L di/dt + R i(t)\} \quad (\text{eqn 2.15})$$

$$E_n(s) = E_s(s) - E_b(s) = (Ls + R) I(s) \quad (\text{eqn 2.16})$$

$$I(s)/E_n(s) = I_s/(E_s - E_b) = 1/(Ls + R) \quad (\text{eqn 2.17})$$

Performing the same operation to the remaining differential equations, the block diagram in Figure 2.2 results.

It is important to note that while a dc motor is basically an open-loop system, the back emf of this type of dc motor acts as a natural feedback loop that tends to improve the stability of the motor.

Once the basic block diagram is developed, writing a CSMP program is simple and fairly straightforward. Care must be taken, however, to put the block transfer functions into the proper format for CSMP's functional blocks. A copy of the CSMP program for a basic dc motor is provided in Appendix A.

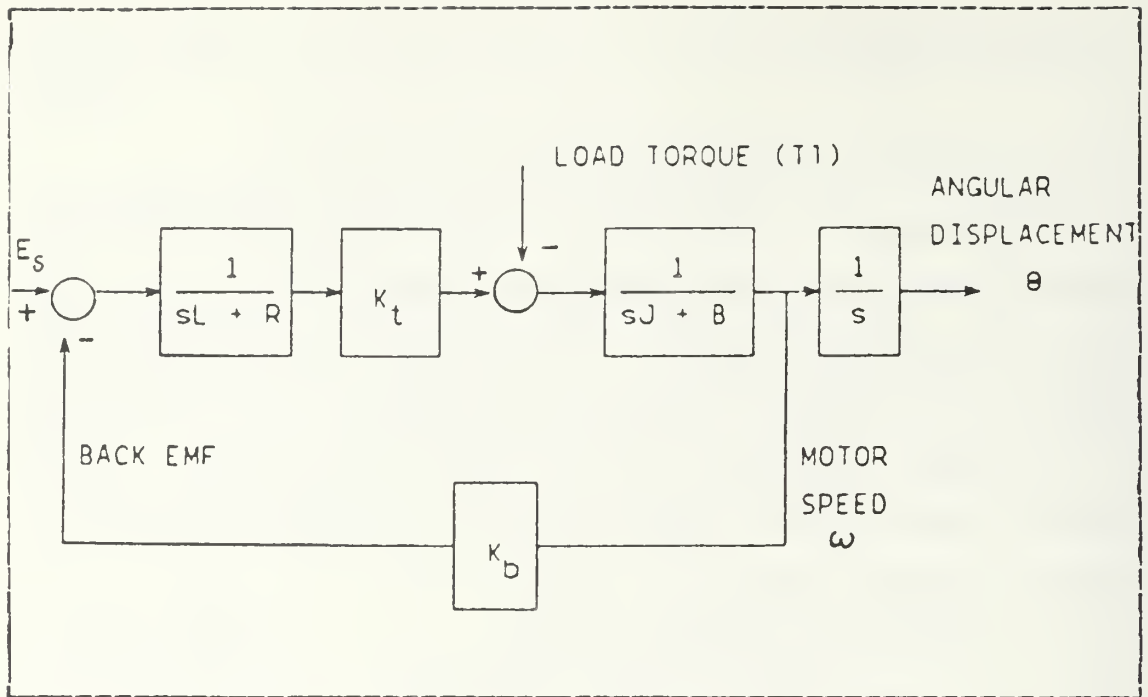


Figure 2.2 Block Diagram of DC Motor

III. CURVE PREDICTION

A. OVERVIEW

One of the purposes of this model is to produce a set of performance curves that accurately simulate a given motor's behavior when operated under varying load conditions. As such the model can be a useful tool for studying the changing performance due to the configuration changes of a motor under development or for observing the behavior of a motor under varying conditions of application or environment. Thus, having developed an input-output computer model for the DC motor, the next step was to assign values to the model parameters and run the program. Program inputs, constants and parameters were assigned values that are typical of brushless DC motors commercially available. Table I provides the parameter values for a given motor that will be used as a generic motor for the following analysis and discussion.

TABLE I
Typical Commercial Motor Parameters

Stator Resistance, R	2.74	ohms
Stator Inductance, L	0.0016	henries
Torque constant, K_t	15.9	oz-in/amp
Back EMF constant, K_b	0.112	volt/rad/s
Rotor Inertia, J_m	0.001	oz-in/s ²
Viscous Friction Coefficient, E_m	unknown	oz-in/rad/s

B. SPEED VS TORQUE CURVE

Specifically, three curves were produced: motor speed vs. generated torque, current vs. torque and output power vs. torque. Since permanent magnet DC motors have linear characteristics, a straight-line curve resulted under all load conditions when the parameters of Table I were inserted into the model and a voltage of 30 VDC was applied. In order to fully understand the individual contributions of the various motor parameters on the speed-torque curve, it was necessary to determine the mathematical relationships between the parameters. Referring to equations 2.1 and 2.5, the electrical and motor equations when considered under steady state conditions become

$$e_s(t) = R \cdot i(t) + K_b \cdot \omega_m(t) \quad (\text{eqn 3.1})$$

$$t_m(t) = K_t \cdot i(t) \quad (\text{eqn 3.2})$$

Solving for $i(t)$ and combining the equations results in

$$e_s(t) = (R/K_t) \cdot t_m(t) + K_b \cdot \omega_m(t) \quad (\text{eqn 3.3})$$

When there is no torque applied to the motor, the current is small enough to neglect and the no-load velocity becomes

$$\omega_{nl} = e_s / K_b \quad (\text{eqn 3.4})$$

Given that the applied voltage is a constant, it is apparent that knowledge of the value of the back emf constant, K_b , will provide the various no-load speeds for any value of applied voltage. On the other hand, in the absence of any known motor specifications, the no-load speed of a given motor can be empirically measured and then the back emf constant, K_b , can be mathematically derived.

Looking next at the slope of the speed-torque curve, it can be seen that whereas one endpoint of the curve terminates at no-load speed, the other ends at stall which is that value of torque which is large enough to literally stop the motor. From equations 3.1 and 3.2, with w_m set to zero the generated torque, $t_m(t)$, at stall is t_s given by

$$t_s = (K_t/R)*e_s \quad (\text{eqn 3.5})$$

Combining equations 3.4 and 3.5, the equation of a straight line for the speed-torque curve results in

$$w_m(t) = w_{n1} - (R_m*t_m(t)) \quad (\text{eqn 3.6})$$

where

$$R_m = R/(K_b*K_t) \quad (\text{eqn 3.7})$$

and R_m is the slope factor for the curve, also called the speed regulation constant. Obviously, changing any or all of the parameters will alter the slope factor, R_m . However, the back emf constant, K_b , and the torque constant, K_t , are strictly related by the common factor, air gap flux, ϕ . In fact, when both constants are put in the MKS system of units, K_b in volt/rad/s and K_t in Nm/amp, then they are equal as equation 3.8 shows.

$$K_b(\text{volt/rad/s}) = K_t(\text{Nm/amp}) \quad (\text{eqn 3.8})$$

Thus, knowledge of either constant provides knowledge of the other. Referring to equation 3.7, it can be seen that the final unknowns are the resistance, R , and the slope factor, R_m . If the resistance, R , is known from manufacturer specification sheets, for example, then the slope, R_m , can be

easily solved. On the other hand, if given an empirically measured speed-torque curve, it is now obvious that the curve not only provides K_b which in turn provides K_t , but it also can provide a derived value for motor resistance, R . Once acquired, the three basic parameters, K_b , K_t and R , were plugged into the CSMP model and the speed-torque curve for a 30 VDC input was generated (see Figure 3.1).

This same procedure can be used to produce a family of speed-torque curves if it is desired to study a motor's performance under different input voltages. Figure 3.2 shows the family of curves produced when the values given in Table I were entered into the model.

C. CURRENT VS TORQUE CURVE

With the speed-torque curve understood, the next task was to repeat the same general procedure for the motor current vs. torque. As a starting point, the equation for the steady-state current is given by

$$i_{ss}(t) = (e_s(t) - K_b \omega_m(t)) / R \quad (\text{eqn 3.9})$$

Since K_b and R were fixed by the speed-torque curve, generating a current-torque curve was a straightforward procedure for any applied voltage (see Figure 3.3).

D. OUTPUT POWER VS TORQUE CURVE

The final performance curve to be studied was the output power vs. torque curve. The basic equation for power is given by

$$P(t) = t_m(t) * \omega_m(t) \quad (\text{eqn 3.10})$$

$$P(t) = K_t * i(t) * \omega_m(t) \quad (\text{eqn 3.11})$$

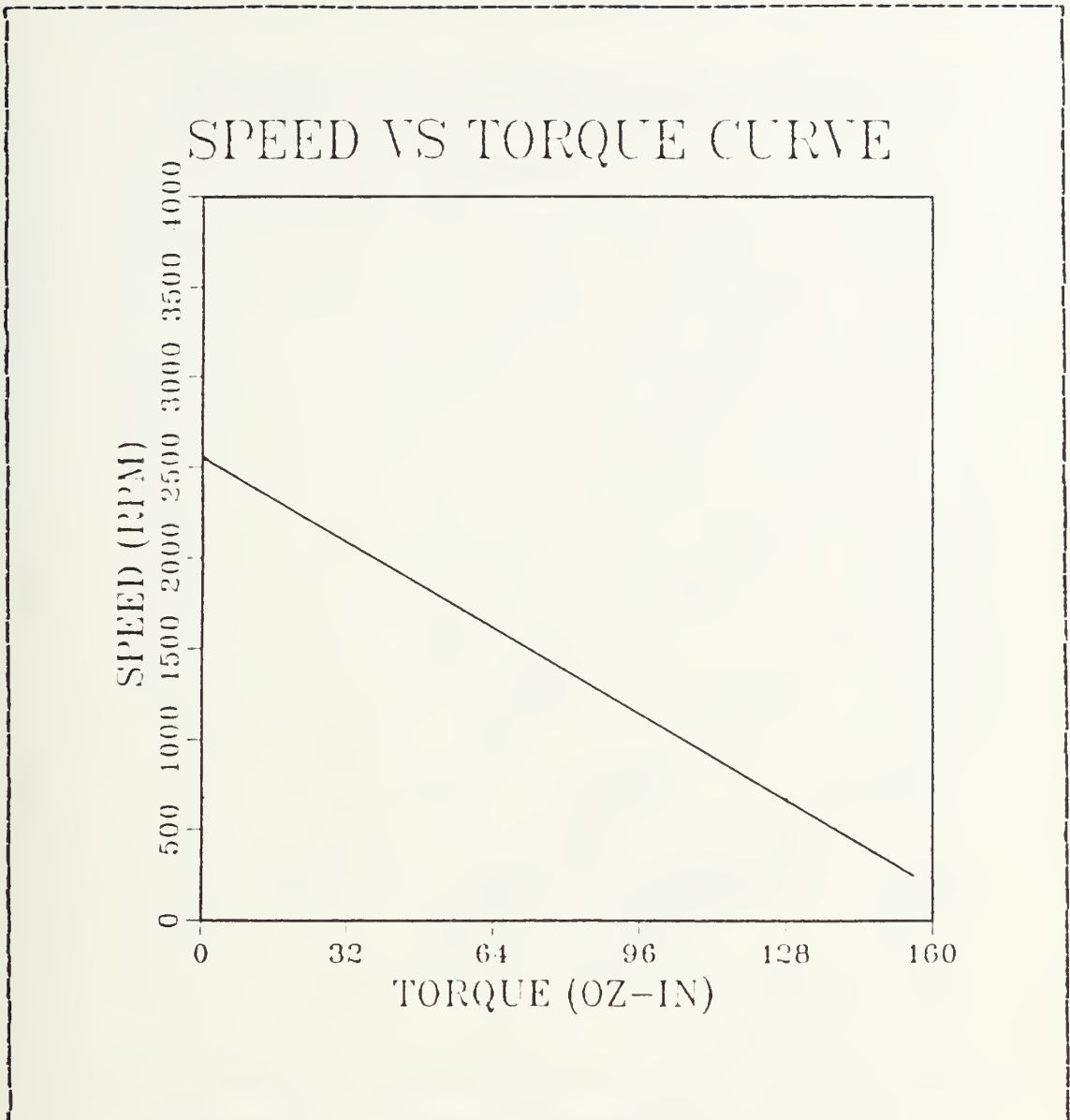


Figure 3.1 Motor Speed vs Torque Curve

where power is measured in watts. Since this equation involves no new constants, producing the power curve was only a matter of adding a line to the existing model which also included a conversion factor for changing the torque units from oz-in/amp to Nm/amp in order for the power to be

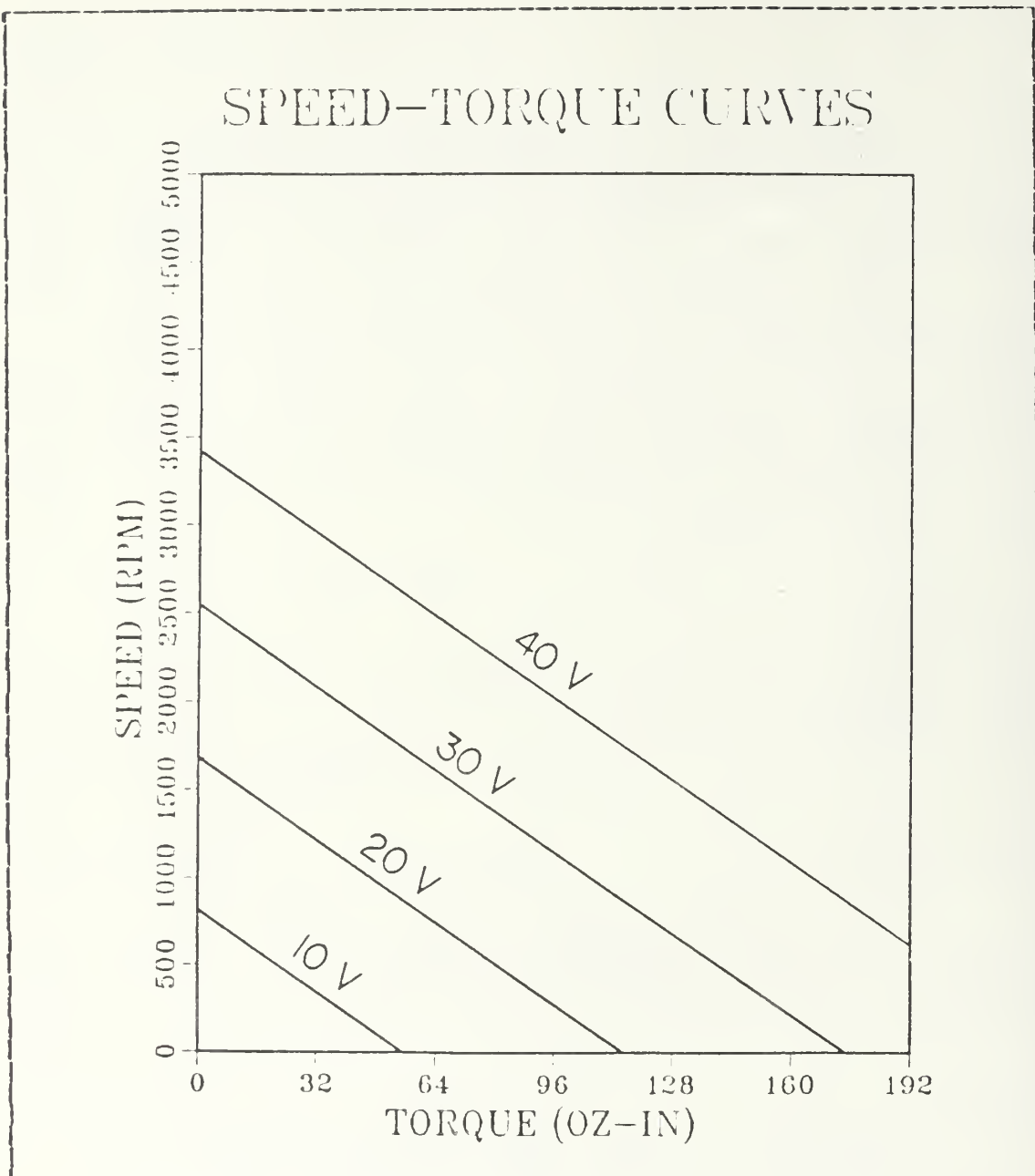


Figure 3.2 Family of Speed-Torque Curves

dimensionally correct in watts. Again running the program with the parameters given in Table I, the model produced the power curve given in Figure 3.4

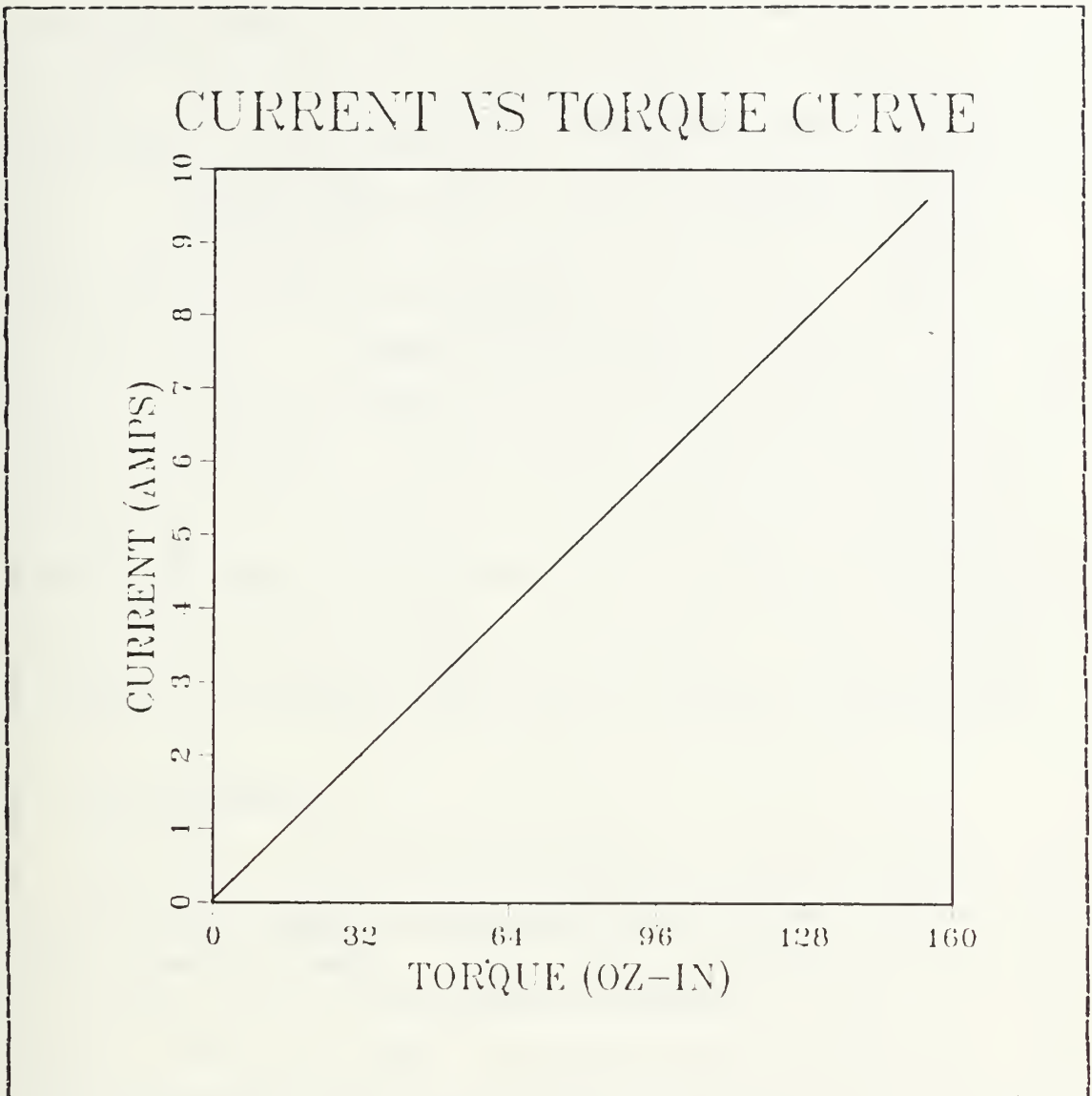


Figure 3.3 Motor Current vs Torque Curve

As expected both the speed-torque and current-torque curves were linear. The power-torque curve is obviously not linear, especially at high loads where the power begins to roll off fairly sharply. From the modelling point of view this is due solely to the fact that the motor slows down faster than the load torque increases (see equation 3.9).

OUTPUT POWER VS TORQUE CURVE

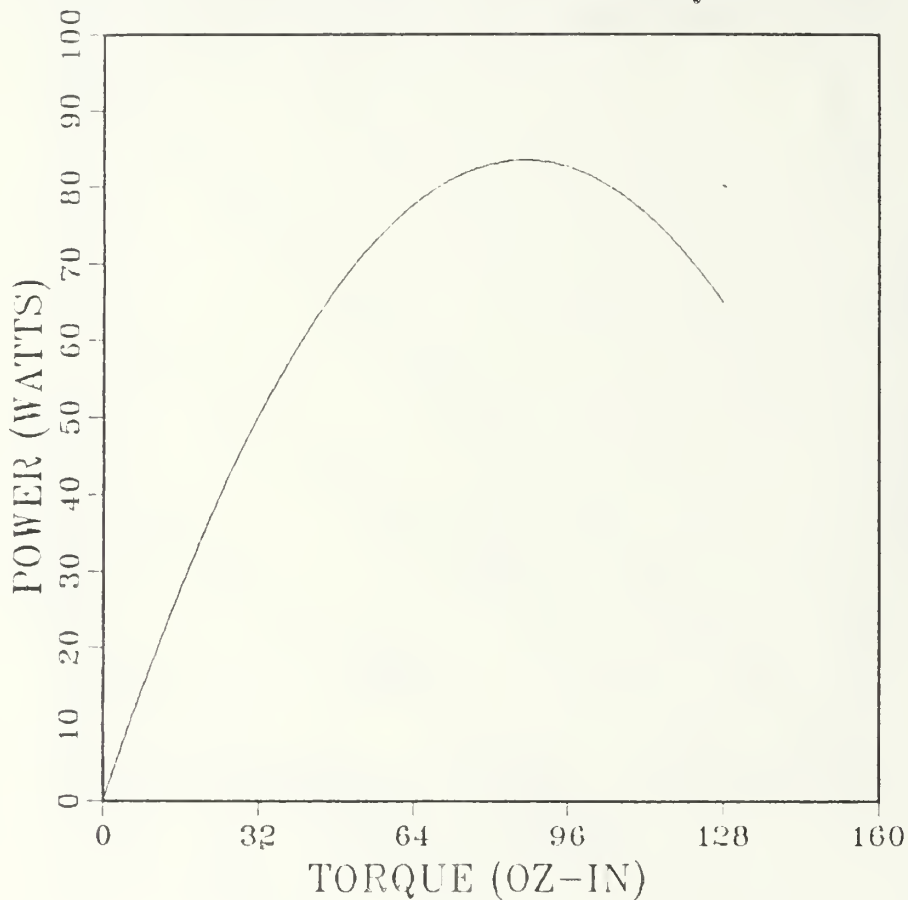


Figure 3.4 Output Power vs Torque Curve

Another factor that further accentuates this power rolloff in an actual motor is the effect due to armature reaction. Whenever a current flows through the motor armature in a permanent magnet dc motor, the armature becomes an electro-magnet which produces a flux that tends to oppose the flux produced by the permanent magnets. This has the effect of

partially demagnetizing the permanent magnets. This demagnetization is a reversible effect, meaning that as current returns to zero the permanent magnets return to their full strength. However, as the current increases and armature reaction sets in, it has the effect of decreasing the torque constant, K_t (as well as K_b). As equation 3.9 indicates, this also contributes to the output power rolloff at high loads. Though current permanent magnet DC motors made of rare earth magnets have high coercivity that resists armature reaction, at high levels of rated current a small amount of armature reaction still occurs. For the purposes of this thesis, the model is considered to accurately simulate motor behavior for loads up to the peak power load for the given applied voltage. From that load upward, it is assumed that armature reaction is likely to occur and result in nonlinear behavior which is not included in this model.

E. MOTOR REVERSAL

The final step in the modeling procedure was to reverse the motor's direction and ensure that mirror images of the three curves resulted. To do this, it was first necessary to replace the positive input voltage with a negative counterpart. Next, in order to maintain model consistency where the load torque, $t_l(t)$, is treated as a torque that opposes the motion of the motor, it was necessary to modify the model so that the load torque was a positive value. This consisted of creating a CSMP procedure block that identified the input voltage as either positive or negative and then treated the load torque accordingly. Once program bugs were removed, the model accurately simulated motor reversal with proper speed, current and power values for the appropriate load conditions.

IV. ELECTRONIC COMMUTATION

A. SWITCHING ACTION

The next major step in this thesis was to convert the basic model of a standard brush-type dc motor into a three-phase, four-pole brushless dc motor system. Figure 4.1 shows this system with the three-phase stator windings configured in a standard 'star' connection with each winding oriented 120 electrical degrees from the others.

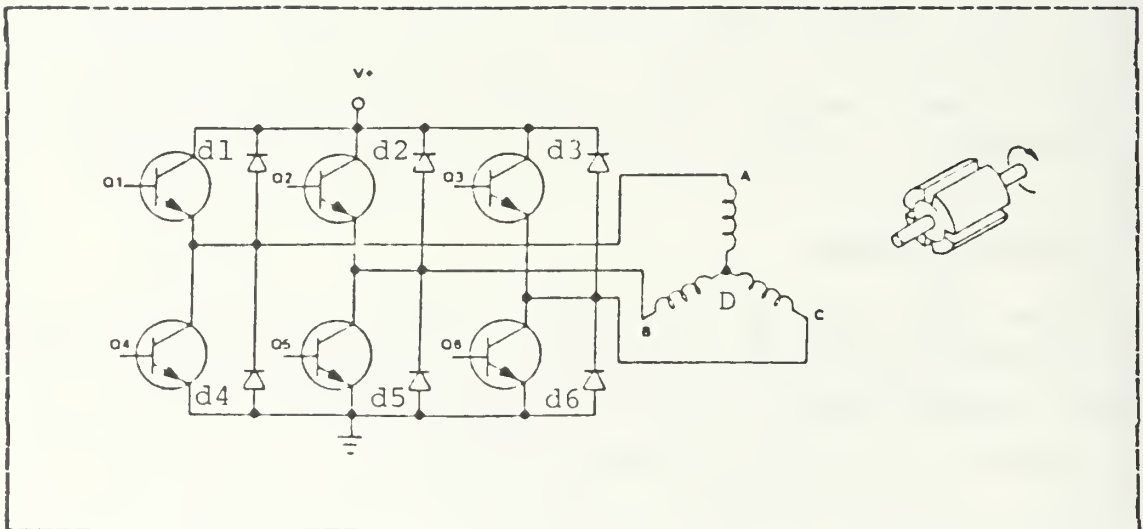


Figure 4.1 Controller Configuration

The six transistors are connected to the ends of each stator leg and through logic-controlled switching action provide three-phase full-wave motor control. Figure 4.2 indicates the switching logic sequence for counterclockwise rotation.

To produce clockwise rotation, the sequence is reversed. In either case, a pair of transistors will be switched at the start of each 30 degree (mechanical) interval which causes current to simultaneously build up in one leg, flow

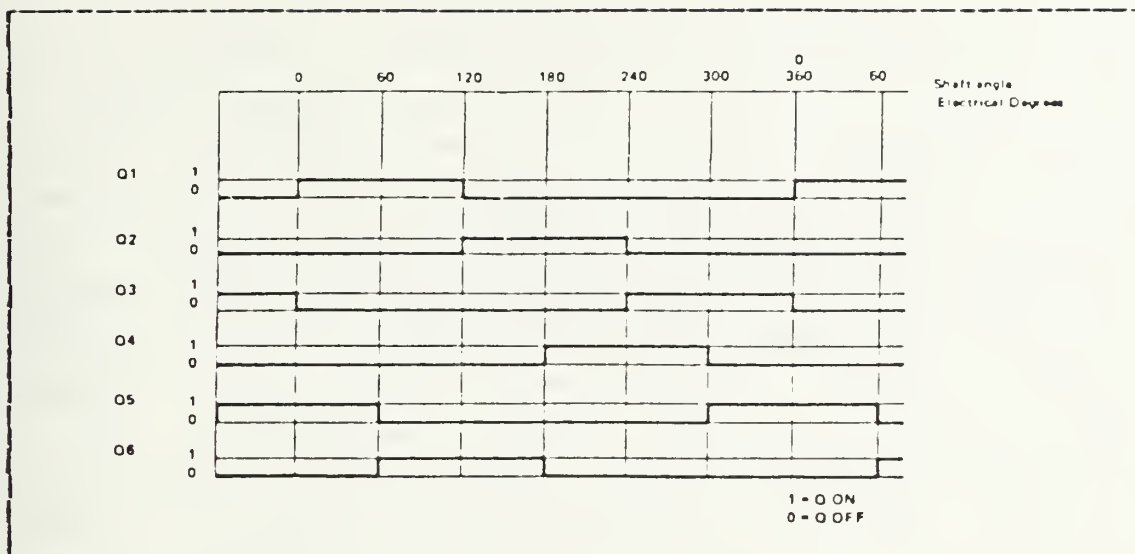


Figure 4.2 Switching Logic of a 3-Phase Brushless DC Motor

steadily in a second, and decay to zero in a third. Given proper sequencing, the net developed torque ideally reaches a steady state value that causes motor rotation at a constant speed in the desired direction.

For windings configured in a star arrangement, it can be seen that conduction is continuous in one leg while commutation occurs in the other two legs. For example, as Q1 and Q5 are energized between 30 and 60 degrees (mechanical), current flows down leg A and into leg B. At the same time, the current through leg C due to the energy storage behavior of an inductor decays to zero through diode, D3 (see Figure 4.1). In the next sequence, 60 to 90 degrees, Q6 is energized and Q5 switched off. Current has reached a steady state flow through leg A, but now it flows down leg C and the current in leg B decays to zero through D2. In the next sequence, 60 to 120 degrees, Q2 is switched on and Q1 switched off. Current has reached steady state flow through leg C but now current builds up and flows from leg B while the current in leg A decays through leg C. This same action

repeats in subsequent commutation states. Looking at point D in Figure 4.1, it can be seen that, since current is always continuous in one leg whether flowing into or from node D, Kirchoff's Current Law requires that the net current flowing in the other two legs must equal the flow in the continuous leg. This permits the following important simplification which was needed later in the modeling process. Namely, the three-legged stator can be approximated by just two windings serially configured. One leg will always accurately reflect steady state flow conditions while the other will be treated as if it were in steady state because the build up in one leg is balanced by decay in the other. It is recognized that this model is a first approximation and that future models will require additional refinements in order to adequately represent the effect of switching transients on the transistor and diode elements.

E. HALL EFFECT SENSOR FEEDBACK

As was mentioned in the introduction, the switching action of the commutation circuitry is based upon rotor position feedback from Hall effect sensors. In order to represent electronic switching and positional feedback, as well as the three phase winding configuration, it was necessary to modify the block diagram of Figure 2.1 to that in Figure 4.3

Comparing Figures 2.1 and 4.3, it is seen that the chief difference is in the switching logic block and the addition of two more transfer function blocks to account for the additional windings. To better understand the logic relationship between the sensors and the current switches, the truth table for both counterclockwise and clockwise rotation is presented in Table II.

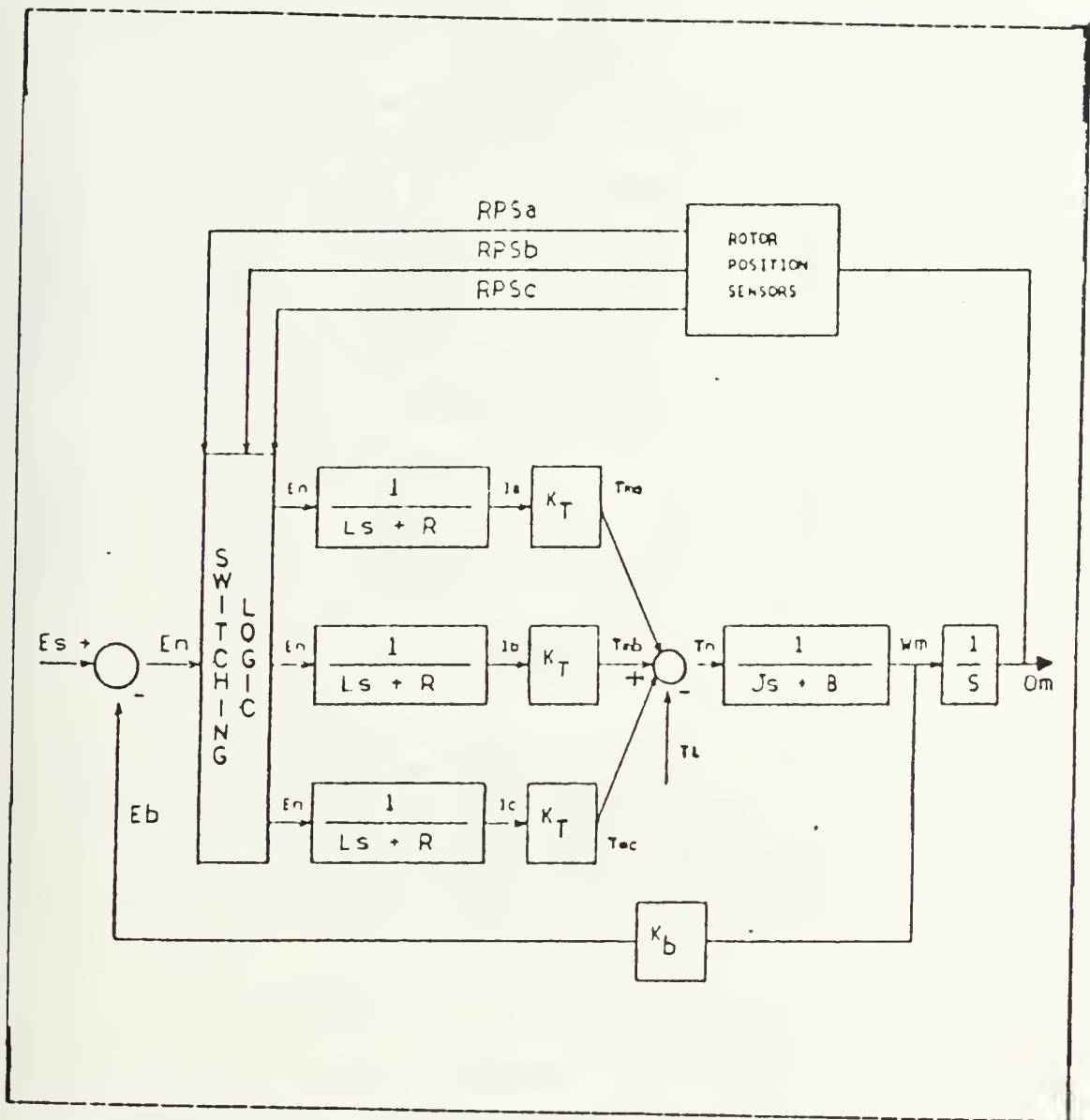


Figure 4.3 Equivalent Circuit With Electronic Commutation.

A brief review of the action of a Hall effect sensor is in order at this point. Consider a conducting material with a constant current flow. When there is no external magnetic field present, the current flows undisturbed in a straight line. But when a magnetic field is applied, a deflecting force, the Lorentz force given by $I \mathbf{l} \times \mathbf{B}$ (where I is the

TABLE II
Sensor and Switching Logic

RPS A	RPS B	RPS C	PH A	PH B	PH C
1	1	0	high	low	open
1	0	0	high	open	low
1	0	1	open	high	low
0	0	1	low	high	open
0	1	1	low	open	high
0	1	0	open	low	high

COUNTERCLOCKWISE

0	0	1	low	high	open
1	0	1	open	high	low
1	0	0	high	open	low
1	1	0	high	low	open
0	1	0	open	low	high
0	1	1	low	open	high

CLOCKWISE

current, l is the length of the conductor and B is the magnetic field) causes the current to bend and electrons to pile up on one side and positive charges, or holes, to do the same on the other side. Thus a transverse Hall potential difference, V_h , develops across the conductor (see Figure 4.4).

Figure 4.5 shows that in the presence of a sinusoidal magnetic field produced by a rotating magnet, such as one of the pole-pairs of a multiple-pole motor, the induced Hall voltage takes on an ideal square wave shape.

The logic circuitry of the sensor is configured in such a way as to output a logic level 1 for positive Hall voltages and a 0 for negative voltages. Briefly reviewing the action of the motor: as the shaft turns, the rotor position sensors send this information to the switching logic block which then decides which phases are to be made high, low or open in accordance with Table II. Equivalently, the voltage, E_n , is then applied to the two appropriate windings

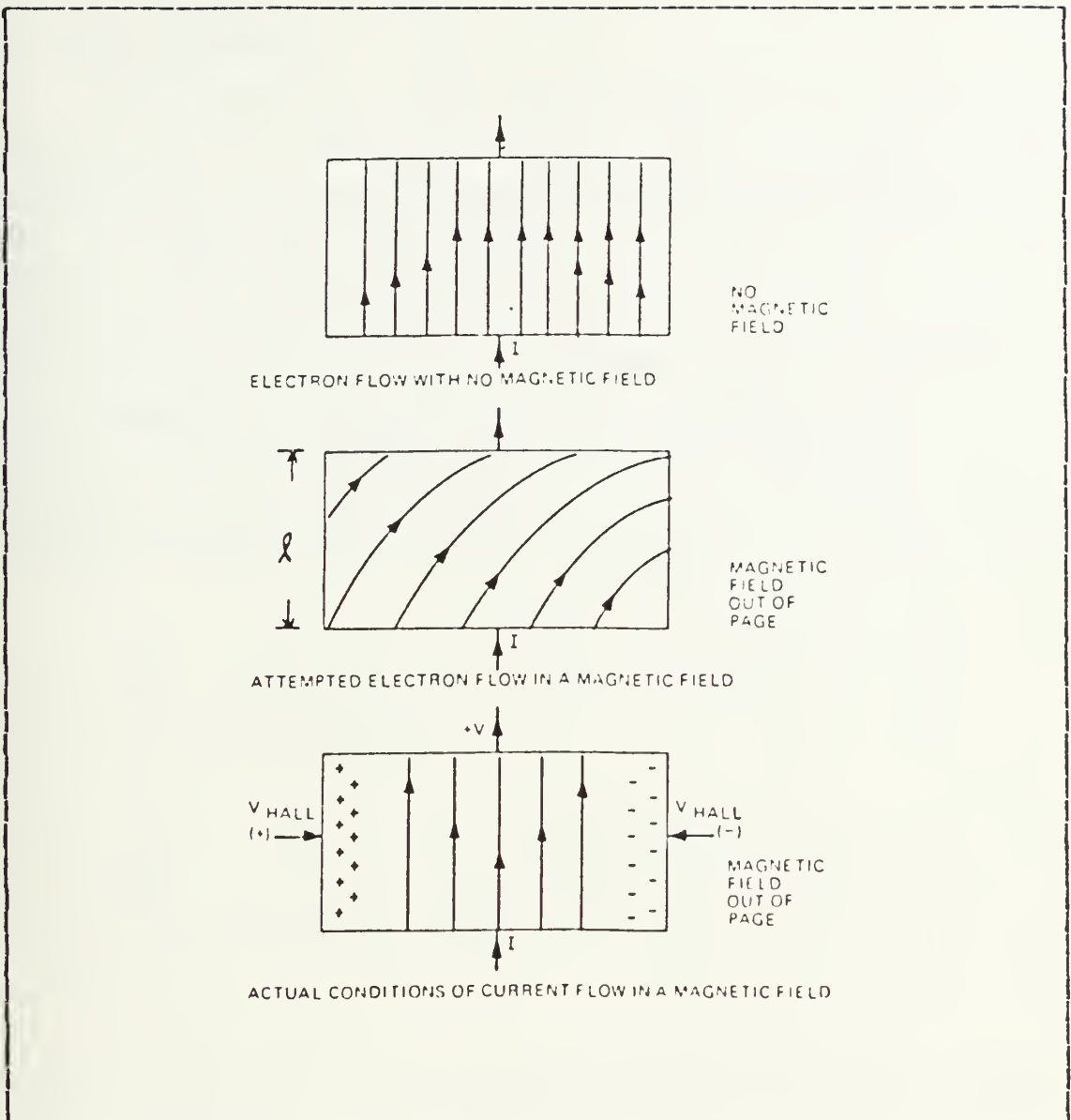


Figure 4.4 The Hall Effect

and zero voltage is applied to the third winding in agreement with the assumption that current is steady in one leg while the commutation in the other two legs is equivalent to a continuous current in one leg. As before, each voltage then produces a current. Because this is assumed to be a

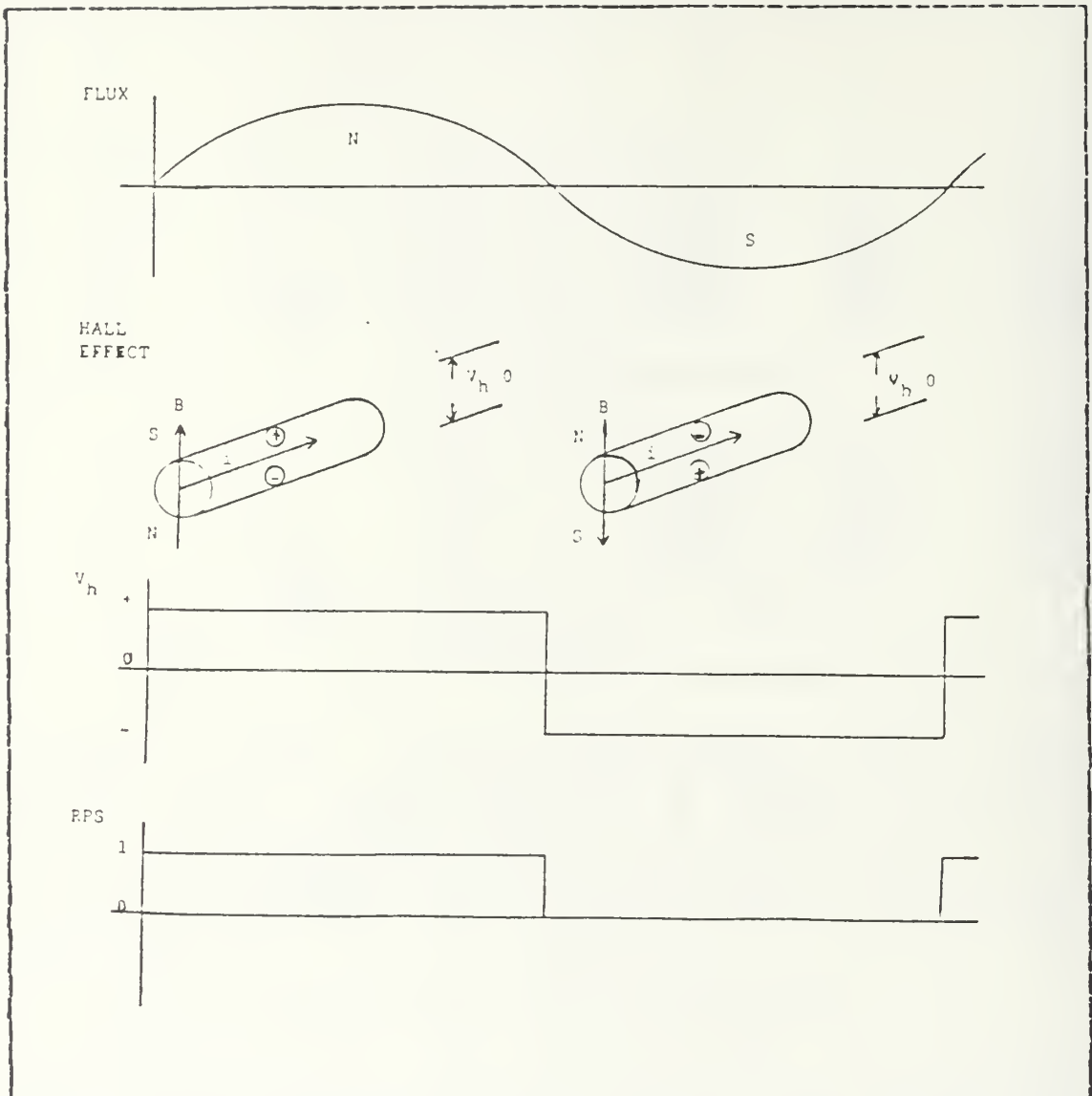


Figure 4.5 Sensor Logic Based on a Hall Effect Sensor

linear system, the principle of superposition is applicable and, thus, the torques developed by current flow through separate windings can be considered independently and then summed to give a total motor torque. Beyond this point, the brushless motor components are identical to its brush-type counterpart and behave similarly.

C. MODEL REVISION

CSMP modeling of this version of the brushless dc motor called for two modifications to the brush-type model. Essentially, a CSMP procedure function was constructed to act as a subroutine that embodies the logic of the switching action. The logic recognizes that if the motor shaft is within some degree range, for example 30 to 60 degrees, then it sets the appropriate rotor position sensors and energizes the switches for the appropriate two windings and deenergizes the switch for the third. In effect, only the forcing voltages are passed to the main program, whereas switch and sensor positions are available for output (see Appendix A).

V. VARIABLE FLUX

A. AIR GAP FLUX

The steady state behavior of both a brush-type and a brushless dc motor has been studied under the fundamental assumption that the back emf generated is a product of the shaft velocity times a constant, K_b (see Equation 2.2). Likewise, the motor torque is equated to the product of the current times a constant, K_t (see Equation 2.12). But as Equation 2.11 reveals in the case of the torque constant, K_t , the torque is in fact the product of some other constant of proportionality, K_{t1} , times the air gap flux, ϕ . The same is true for the back emf constant, K_b ; that is, K_b is the product of some proportionality constant, K_{b1} , times the air gap flux, ϕ . In both cases, the flux, ϕ , has been assumed to be constant which is in agreement with the general practice when modeling permanent magnet dc motors. In point of fact, the flux is not constant but rather is distributed sinusoidally, generally being the sum of a sinusoid and one or more of its harmonics. How the motor is physically constructed determines this flux distribution. Two of the chief factors are the structure of the magnetic pole faces and, most importantly, how the windings are distributed in the armature. The latter includes such factors as the number of slots, the number of coils per slot and the spacing of the slots [Ref. 5]. The careful designer distributes the windings so as to minimize the effects of harmonics. Regardless of their constituents, these composite sinusoids have an average value, of course, and so in practice it is this average value that becomes the constant flux term, ϕ .

B. FLUX AS AN AVERAGE VALUE

A logical next step in the design of a more realistic model was the determination of an average value for the variable flux, ϕ_{avg} , and the corresponding proportionality constant, $KK1$ such that the ratio of ϕ_{avg} and $KK1$ equals one and the relationships of equations 2.2 and 2.5 are preserved. The equations for back emf, $e_b(t)$, and developed torque, $t_m(t)$, now become

$$e_b(t) = K_{bp} * \omega_m(t) \quad (\text{eqn 5.1})$$

$$t_m(t) = K_{tp} * i(t) \quad (\text{eqn 5.2})$$

where the back emf constant, K_{bp} , and the torque constant, K_{tp} , are now expressed as

$$K_{bp} = K_b * (\phi_{avg}/KK1) \quad (\text{eqn 5.3})$$

$$K_{tp} = K_t * (\phi_{avg}/KK1) \quad (\text{eqn 5.4})$$

Assuming as a first approximation that the air gap flux varies as a simple sinusoid of unit magnitude, the first step toward finding the total system flux, ϕ_{avg} , was to determine the relationship of the individual flux patterns in each of the three phase windings. Analysis of a four-pole magnet rotating under three windings separated by 120 degrees (electrical) revealed the following relationships

$$\phi_a = \sin(2\theta + \pi/6) \quad (\text{eqn 5.5})$$

$$\phi_b = \sin(2\theta + 9\pi/6) \quad (\text{eqn 5.6})$$

$$\phi_c = \sin(2\theta + 5\pi/6) \quad (\text{eqn 5.7})$$

where ϕ_a , ϕ_b and ϕ_c are the flux contributions of the respective phases. Returning to an earlier assumption that the circuit can be approximated as two windings in series, ignoring the third, then the average flux can also be approximated from the sum of the flux developed in two windings at a time. This approximation is further supported by the fact that the flux in the decay leg has, in fact, an average value of zero during every commutation interval. From the switching sequence of Figure 4.1, the two conducting legs were identified for each interval and, from Equations 5.5 through 5.7, their respective flux values calculated and summed. For every interval, the resulting flux waveshape was identical and had an average value of $\phi_{avg} = 1.631$ (see Figure 5.1).

Since KK1 merely normalizes ϕ_{avg} , its value was easily determined to be $KK1 = 0.613$. The appropriate substitutions were then made in the CSMP model (see Appendix A for Revision Two). Since this amounted to nothing more than a rearrangement of constants, the model's output behavior remained unchanged. At this stage, the model simulates the behavior of a brushless dc motor being electronically commutated and exhibiting constant, steady state developed torque and motor speed due to a fixed, average value air gap flux.

C. SINUSOIDAL FLUX

The final stage of this thesis was to examine the steady state behavior of the brushless dc motor under variable air gap flux conditions. As a first approximation, the flux was modeled as a simple sinusoid and the flux relationships are those given in equations 5.5 through 5.7. As before, only the flux relating to the two conducting legs was considered. This composite variable flux, ϕ_{v1} , is shown in Figure 5.1. Equations 5.3 and 5.4 had to be modified to account for the different value of flux.

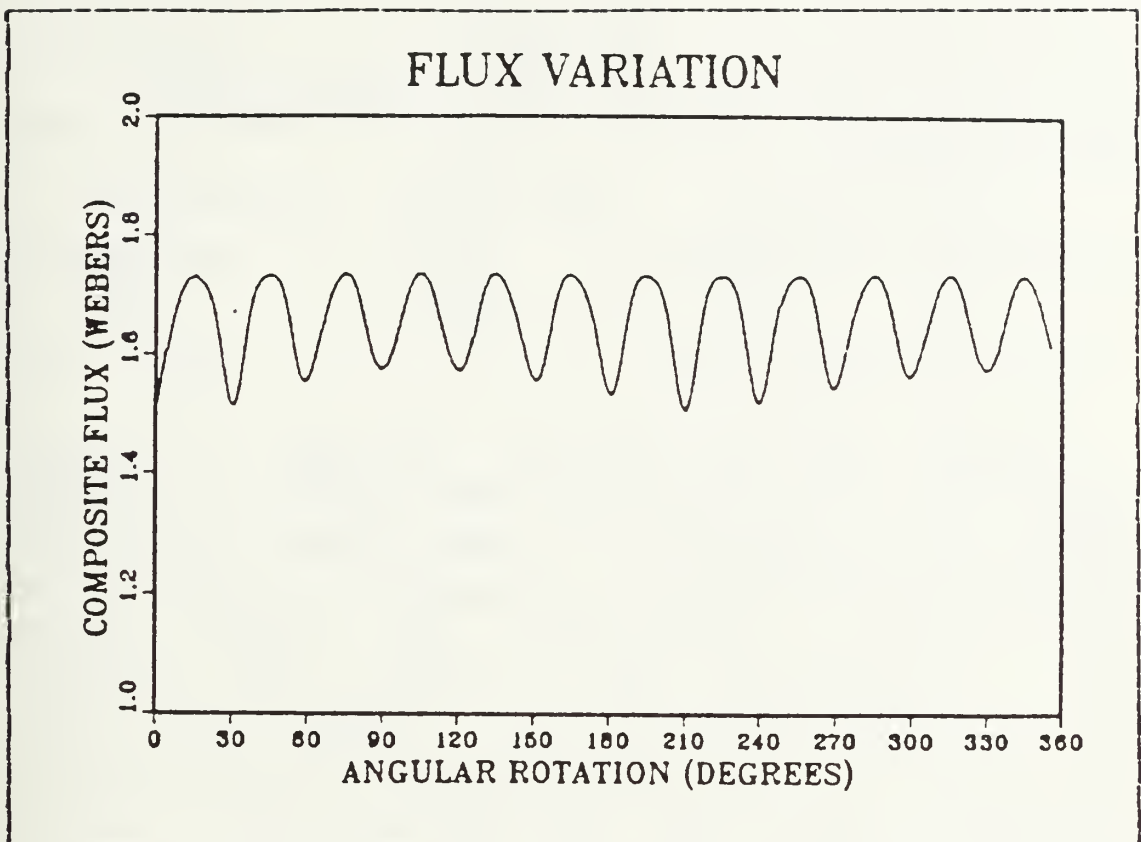


Figure 5.1 Composite Flux Variation for Two Windings

$$K_{bpp} = K_b * (\phi_{v1}/KK2) \quad (\text{eqn 5.8})$$

$$K_{tpp} = K_t * (\phi_{v1}/KK2) \quad (\text{eqn 5.9})$$

Recall that the objective was to keep the values of K_{bpp} and K_{tpp} as near as possible to those of K_b and K_t , respectively. In order to roughly normalize ϕ_{v1} , the constant value was determined as $KK2 = 1.655$. Since ϕ_{v1} was now a variable quantity, it should be recognized that K_{bpp} and K_{tpp} were no longer strictly constants and were better expressed as the following functions.

$$K_{bpp} = K_b(\phi_{v1}) \quad (\text{eqn 5.10})$$

$$K_{tpp} = K_t (\Phi_{v1}) \quad (\text{eqn 5.11})$$

The equations for back emf, $e_b(t)$, and developed torque, $t_m(t)$, now became

$$e_b(t, \Phi_{v1}) = K_{bpp} * \omega_m(t) \quad (\text{eqn 5.12})$$

$$t_m(t, \Phi_{v1}) = K_{tpp} * i(t) \quad (\text{eqn 5.13})$$

Because the total flux was no longer a constant, average value, it was expected that variation in developed torque (and, consequently, in motor speed) would result. Furthermore, as the system block diagram of Figure 2.1 indicates, torque is converted by the motor transfer function into a rotational speed. This is a process that is equivalent to inertia filtering of the torque ripple that results from variable flux. For the purposes of this thesis, ripple is defined as the ratio of the amount of variation from the maximum to the maximum itself. Having made the appropriate substitutions in the model (see Appendix A for Revision Three), the program was run under no-load conditions. It was observed that there was, in fact, ripple in both the developed torque and motor speed and that some inertia filtering did occur. The next logical step was to load the motor and study the effect on torque and speed ripple. Table III indicates that under no-load conditions where speed was highest, the percentage of ripple in the output speed was at a minimum but that torque ripple was at a maximum.

It can be seen that as the load increased the amount of ripple in the developed torque decreased from about 84% to 8%. A closer examination of the torque behavior under varying loads revealed that, even as the motor torque necessarily grew with increasing loads, in every case there was

TABLE III
Torque and Speed Ripple Due to Sinusoidal Flux

MOTOR LOAD (oz-in)	MOTOR SPEED (RPM)	% RIPPLE	
		TORQUE	SPEED
0.0	2557	83.9	1.1
32.0	2087	21.1	1.6
64.0	1617	12.2	2.6
96.0	1147	7.8	4.6

approximately a constant 8-9 oz-in variation. This variation can be attributed primarily to the flux variation in K_{tp} and to a lesser degree to the variation in $i(t)$ caused by the variation in back emf. Thus the magnitude of torque variation remained about the same for all loads though the percentage ripple appears to indicate otherwise. In the case of motor speed, the amount of ripple appeared to increase slightly with increasing load and thus decreasing speed. In this instance, the magnitude of variation did increase a small amount with decreasing speed - from 28 rpm at no-load to 52 rpm at 96 oz-ins - and suggests that speed ripple, at least, is somewhat dependent on load. This is due in part to the fact that as the motor slows, there is less rotor momentum and thus less inertia filtering. In addition, at slower speeds there are less frictional effects which at higher speeds also tend to filter out ripple. In general, it makes intuitive sense that at higher speeds frequency variations are harder to discern than at slower speeds.

D. HARMONIC FLUX

Having observed the effects of simple sinusoidal flux variation, the next step was to replace the single sinusoid with a flux composed of the sum of a sinusoid and its harmonics which is more representative of the air gap flux

patterns in an actual motor. The back emf of a typical commercial brushless dc motor is given in Figure 5.2 where the voltage between two terminals was measured with the motor rotating at 1200 rpm.

A harmonics analysis of this waveshape shows that the principle harmonic was the fifth and that the waveshape was closely described by the expression

$$3.0 \sin(\theta) + 0.59 \sin(5\theta) \quad (\text{eqn 5.14})$$

When substituted into equations 5.5 thru 5.7, and the different angular speed taken into account, the following relationships for flux result

$$\phi_a = 3.0 * \sin(2\theta + \pi/6) + 0.59 * \sin(10\theta + 5\pi/6) \quad (\text{eqn 5.15})$$

$$\phi_b = 3.0 * \sin(2\theta + 9\pi/6) + 0.59 * \sin(10\theta + 9\pi/6) \quad (\text{eqn 5.16})$$

$$\phi_c = 3.0 * \sin(2\theta + 5\pi/6) + 0.59 * \sin(10\theta + \pi/6) \quad (\text{eqn 5.17})$$

The same procedures used in the simple sinusoid model were then applied to the harmonics case where the composite flux changes to ϕ_{v2} , a flux factor that varied to a slightly greater degree than did ϕ_{v1} . Equations 5.8 and 5.9 had to be modified as follows

$$K_{b\text{ppp}} = K_b * (\phi_{v2}/KK3) \quad (\text{eqn 5.18})$$

$$K_{t\text{ppp}} = K_t * (\phi_{v2}/KK3) \quad (\text{eqn 5.19})$$

where $KK3$ approximately normalizes the flux and had the value $KK3 = 5.38$. As before, $K_{b\text{ppp}}$ and $K_{t\text{ppp}}$ varied with the flux and so the new equations for back emf and developed torque became

BACK EMF WAVEFORM

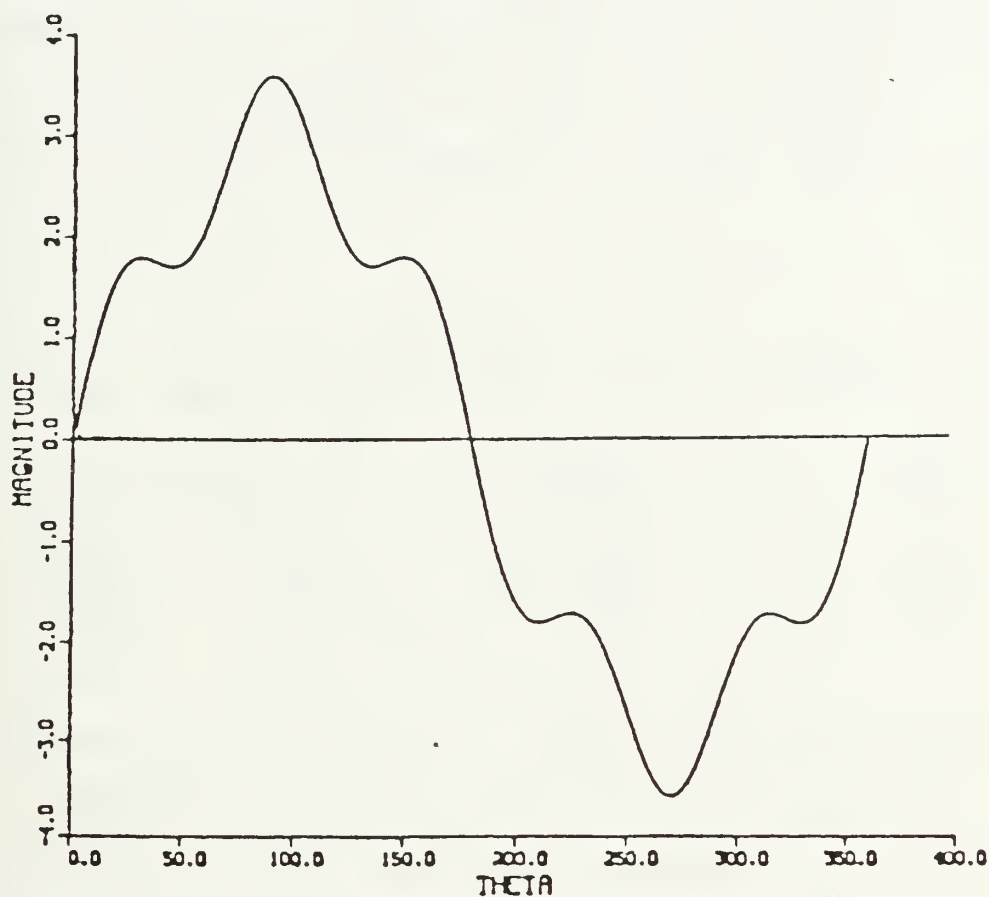


Figure 5.2 Back EMF Waveform Due to Harmonic Flux

$$e_b(t, \phi_{v2}) = K_b(\phi_{v2}) * w_m(t) \quad (\text{eqn 5.20})$$

$$e_b(t, \phi_{v2}) = K_{b\text{ppp}} * w_m(t) \quad (\text{eqn 5.21})$$

$$t_m(t, \phi_{v2}) = K_t(\phi_{v2}) * i(t) \quad (\text{eqn 5.22})$$

$$t_m(t, \phi_{v2}) = K_{tppp} * i(t) \quad (\text{eqn 5.23})$$

The appropriate substitutions were once more made in the model (see Appendix A for Revision Four) and the model was run under various loads. As anticipated, the variable flux, ϕ_{v2} , produced ripple in the developed torque and motor speed. Table IV shows the resultant values for various loads.

TABLE IV
Torque and Speed Ripple Due to Harmonic Flux

MOTOR LOAD (oz-in)	MOTOR SPEED (rpm)	% RIPPLE	
		TORQUE	SPEED
0.0	2557	94.6	2.4
32.0	2087	38.5	3.7
64.0	1617	22.5	5.6
96.0	1147	14.7	9.8

Comparing Tables III and IV, it can be seen that the values for torque and speed ripple are of similar magnitudes. The somewhat higher values for torque are due to the fact that in the ϕ_{v2} case there was a 16-21 Oz-in variation as opposed to an average 8-9 oz-in variation in the ϕ_{v1} case. The speed ripple behavior was much like the ϕ_{v1} case with proportionate increases resulting from the increased torque ripple. Thus, for both torque and speed ripple due to ϕ_{v2} , the model performed as expected; that is, slightly higher values of ripple occurred which were clearly attributable to the increased variability of the flux pattern of composite sinusoidal harmonics.

An important observation made during runs of the ϕ_{v1} model came as a consequence of the motor speed variability,

particularly when the motor was unloaded. Since no-load speed was a function of K_b as given in equation 3.4, the variable K_{bpp} had the effect of increasing the upper-end speed beyond the 2557 rpm baseline given in Figure 3.1. This increased magnitude coupled with the swing of speed values created an undesirable effect in the unloaded condition. In effect, at certain points in time the additional speed produced back emf values that exceeded the input voltage which in turn resulted in negative current and developed torque values. Though these were transient negative values and had small effect on the steady state operation of the motor, still their presence was obviously unrealistic. The solution to returning the motor to all positive values of current and torque was to increase the friction filtering effect by adjustment of the viscous friction coefficient, B_m . It will be recalled from Chapter Three that a value for the B_m of the commercial motor being modelled was not available and that for the basic model a value for B_m was derived from the curve fitting process. Thus, it seemed reasonable and permissible to repeat the procedure here.

Since it makes sense that increasing the friction within a system will slow the system down, in this case increasing the value of B_m did just that. By increasing B_m from 0.00015 to 0.045 oz-in/rad/s, the upper-end of the motor speed was reduced to a value that eliminated the undesirable negative values. This caused the no-load speed to be lowered slightly below the desired value of 2557 rpms. Recalling that no-load speed is fixed by the back emf constant, K_b , this parameter was adjusted from 0.1120 to 0.1089 vclt/rad/s to bring the back up to speed. Since this adjustment was less than 3% and the manufacturer specifications allowed a 10% +/- measurement error margin, this adjustment to K_b was permissible. Of course, a proportionate adjustment to the torque constant, K_t , was also made

since K_t and K_b must maintain a constant relationship as explained in Chapter Three. The effect on motor speed ripple was negligible. Reviewing the ϕv_2 model at this point revealed that similar behavior in the no-load state occurred but on a larger scale due to the greater variability of ϕv_2 . A similar set of adjustments was necessary to eliminate the negative current and torque values in the unloaded condition. It required an adjustment of B_m from 0.00015 to 0.045 oz-in/rad/s in order to ensure that all values were positive. In addition, the back emf constant, K_b , was adjusted to 0.1192 volt/rad/s and a proportionate adjustment to K_t was made. Again, all adjustments were within tolerances.

Of course, it was earlier established in Equation 3.7 that changes to K_b and K_t would change the slope of the speed-torque curve. Thus, in both cases the slope was returned to its original value by adjusting the motor resistance, R . In the case of sinusoidal variable flux, R was reduced from 2.74 to 2.70 ohms. For harmonic variable flux, R was increased from 2.74 to 3.0 ohms. Again, both adjustments were within the 10% +/- allowable deviation. It was also observed that since both K_b and K_t no longer remained constant but rather varied within small ranges, the slope was not constant and varied accordingly in both the ϕv_1 and ϕv_2 models with the greatest change occurring when K_b and K_t simultaneously reached the minimum values of their respective ranges. Bearing in mind that these deviations in slope are fairly transient, their average values are most important and are the approximate values from which the final adjustments to R were based.

VI. SUMMARY

A. REMARKS AND CONCLUSIONS

CSMP language is a convenient tool for modeling a brushless DC motor. Positional sensor feedback and switching logic being functions of time, the action of electronic commutation can be nicely simulated in CSMP. The model can be fairly easily modified in order to study other motor configurations. For example, the three-phase star configuration used in this thesis could easily be changed to a grounded neutral, point D in figure 4.1, and the same types of analysis performed. In future studies where the complexity of the model is increased in order to include more design detail, the advantage of CSMP will become even more apparent.

In the course of simulating the effects of different air gap flux variations, it appeared necessary to make minor parameter adjustments in order to offset the feedback effects of torque and speed ripple. Within the scope of this thesis, adjusting the steady state performance was reasonable and justifiable. In a larger context, however, various control systems, particularly torque generation controllers, are specifically designed to reduce torque ripple and its effects. So, in at least one sense, these adjustments were somewhat artificial. To the extent that parameter adjustment is necessary and desirable, it must be understood that this is not a simple procedure since adjustment of one parameter almost always requires adjustment of one or more others. These adjustments in turn necessitate readjustment of the original parameter. The process is thus an iterative one. This model permits this kind of parameter

adjustment, but it is a long and tedious process that would be better performed by some sort of optimization algorithm.

B. RECOMMENDATIONS FOR FUTURE STUDY

The simulation of ripple effects is particularly relevant to the control engineer who must design the control circuitry and power conditioner to meet specific performance requirements. This points to several areas for future study. One area is the control of torque generation and the several principle configurations used in brushless DC motors. Two commonly used methods are the sinusoidal torque generation principle and the trapezoidal torque scheme. [Ref. 5]. In addition to torque generation control, a second area for investigation is power control of brushless DC motors. In this thesis, output power was unregulated and was studied simply as a function of a constant input voltage. In practice, however, power is produced and controlled by varying the supply voltage. Various schemes exist for power control; among these are linear transistor control and pulse-width or pulse-frequency control. [Ref. 5].

A very important area that this thesis did not address was that of the switching transients that occur as a consequence of commutation. During each switching interval, each winding is an inductor that stores energy which causes a significant amount of current to flow at the instant of switching. This can have serious effects, especially if breakdown conditions exist among the commutation transistors and other control circuit elements. In this same area, switching transients also occur within the control circuitry itself. Thus, a thorough investigation and understanding of the behavior of power transistors, diodes and other control elements used with electronic commutation needs to be done.

APPENDIX A
LISTING OF MODEL PROGRAMS

A. BASIC PROTOTYPE MODEL

The program in this section is a basic program that simulates the action of a standard brush-type DC motor. It is the prototype from which the brushless DC motor model and its several revisions are derived.


```

//THCCSMPL JCE (2672,0116), 'THOMAS-LAB6', CLASS=C
//*MAIN QRG=NFGVM1.2672P
// EXEC CSMPXV
//X.CCPRINT CC CUMMY
//X.CCPRINT CC CUMMY
//X.SYSIN DD *

* VERSION ONE -- THIS IS THE BASIC PROGRAM THAT SIMULATES A
* STANDARD BRUSH-TYPE DC MOTOR. IT IS THE
* PROTOTYPE FROM WHICH ALL LATER BRUSHLESS
* DC MOTOR MODELS ARE DERIVED.

INITIAL
CONSTANT KT = 15.5, BM = 0.00015, BL = 0.0, JL = 0.0, ...
N = 1.0, JM = 0.001, KB = .112, PI = 3.14159265
PARAMETER LA = .0016, RA = 2.74, ...
TL = (0.0, 22.0, 64.0, 96.0, 128.0)

KT -- TORQUE CONSTANT (CZ-IN/AMP)
KB -- BACK EMF CONSTANT (VCLT/RAD/S)
RA -- RESISTANCE OF THE MOTOR (OHM)
BM -- VISCUS FRICTION COEFFICIENT OF THE MOTOR
BL -- (CZ-IN/RAD/S)
BLF -- VISCUS FRICTION COEFFICIENT OF THE LOAD
B -- TOTAL VISCUS FRICTION COEFFICIENT OF THE LOAD THRU
JM -- INERTIA OF THE MOTOR (OZ-IN/S-S)
JL -- INERTIA OF THE LOAD
JLF -- INERTIA OF THE LOAD THRU REDUCTION GEARS
JL -- TOTAL INERTIA OF THE MOTOR SYSTEM
TL -- LCAD TORQUE (OZ-IN)
A1 = LA/RA -- THE ELECTRICAL TIME CONSTANT OF THE MOTOR
A2 = JM/BM -- THE MECHANICAL TIME CONSTANT OF THE MOTOR

NOSORT
BLF = BL/(N**2)
JLF = JL/(N**2)
B = BM + BLF
J = JM + JLF
A1 = LA / RA
A2 = JM / BM
THRST = 0.0
JFAC = 0.0

```



```

DYNAMIC 30.0 * STEP(0.0)
VI = VI - VEMF
VIN1 = VIN1 * (1.0/RA)
IM = REALPL(C.0,A1,VIN2)
TM2 = IM * K1
TN2 = TN1 * (1.0/BM)
WMRPM = REALPL(0.0,A2,TN2)
WMPM = WM * KE
VEMF = INTGRL(C.0,WM)
PWR = WM * IM * .0070615

```

```

* THIS PROCEDURE PROVIDES A SIMPLE MECHANISM FOR REVERSING
* THE MOTOR'S DIRECTION

```

```

PROCEDURE IN1=FACBWD(VIN,TM,TL)
IF (VIN.LT.C.0) GO TC 10
TN1 = TM - TL
GO TC 15
10 TN1 = TM + TL
15 CONTINUE
ENDPROCEDURE

```

51

```

* THIS PROCEDURE RESETS THE VARIABLE THRST TO 0 AFTER EVERY 360 DEGREES
* OF MECHANICAL ROTATION. THIS IS FUNDAMENTAL TO THE SIMULATION OF ALL
* SWITCHING AND POSITION SENSING ACTION.

```

```

PROCEDURE THRST=RESET(JFAC,THDEG)
TS = JFAC * 360.0
THRST = THDEG - TS
IF (THRST.LT.360.0) GO TC 40
JFAC = JFAC + 1.0
40 CONTINUE
ENDPROCEDURE

```

```

TERMINAL BASIC CC MOTOR SYSTEM
TITLE FINTIM = .04, CUTCEL = 0.0004, PRCEL = 0.0004
PRINT VEMF, IM, TM, WM, WMPM, PWR
PAGE ENCL
STOP

```

```

ENDJCB
/*

```

B. REVISION ONE

This is the first revision of the basic prototype. This model simulates the switching logic of a brushless DC motor which is based on feedback from Hall effect sensors. In addition, the windings are treated independently and their contributions to developed torque are superposed. Since the superposition results in twice as much current flow as a single lumped coil, the total current is halved to retain the same overall motor behavior as in the prototype.

VERSION TWO -- THIS IS THE FIRST REVISION OF THE BASIC PROTOTYPE. THIS
MODEL SIMULATES THE SWITCHING LOGIC OF A BRUSHLESS DC
MOTOR WHICH IS BASED ON FEEDBACK FROM HALL EFFECT
SENSORS AS DESCRIBED IN CHAPTER FOUR. IN ADDITION,
THE WINDINGS ARE TREATED INDEPENDENTLY AND THEIR
CONTRIBUTIONS TO DEVELOPED TORQUE ARE TREATED AS
SUPERPOSABLE. SINCE THE SUPERPOSITION RESULTS IN
THE TOTAL CURRENT FLOW AS A SINGLE LUMPED COIL,
THE TOTAL CURRENT IS HALVED IN ORDER TO KEEP THE
OVERALL BEHAVIOR THE SAME AS IN VERSION ONE.

```

-- TORQUE CONSTANT (OZ-IN/AMP)
-- BACK EMF CONSTANT (VCLT/RAD/S)
-- RESISTANCE OF THE MOTOR (OHM)
-- VISCCLS FRICTION COEFFICIENT OF THE MOTOR (OZ-IN/RAD/S)
-- VISCCLS FRICTION COEFFICIENT OF THE LOAD
-- VISCCLS FRICTION COEFFICIENT OF THE MOTOR THRU REDUCTION GEARS
-- VISCCLS FRICTION COEFFICIENT OF THE MOTOR SYSTEM
-- VISCCUS FRICTION (OZ-IN/S-S)
-- INERTIA OF THE LOAD
-- INERTIA OF THE MOTOR THRU REDUCTION GEARS
-- INERTIA OF THE LOAD MOTOR TIME CONSTANT OF THE MOTOR
-- INERTIA OF THE ELECTRICAL TIME CONSTANT OF THE MOTOR
-- LA/RA -- THE MECHANICAL TIME CONSTANT OF THE MOTOR
A2 = J/E

```

53

```
THRST = 0.0
JFAC = 0.0
```

```
DYNAMIC
VIF= 30.0 * STEP(0.0)
VIB = C.0
VIN = VIF + VIB
VIN1 = VIN - VEMF
VIN2 = VIN1 * (1.0/RA)
IMA = REALPL(0.0,A1,VA)
IMC = REALPL(0.0,A1,VB)
IMT = REALPL(0.0,A1,VC)
IMT = (IMA + IME + IMC)/2
IM = IMT * KI
IN1 = IN1 * (1.0/B)
IN2 = REALPL(0.0,A2,IN2)
WMRPM = WM * (30./PI)
WMRPMR = WMRPM/N
VEMF = WM * KB
THETA = INTGRL(C.0,WM)
THCEG = THETA * (180.0/PI)
THCCN = THRST
PWR = WM * IM * .0070615
```

* THIS PROCEDURE PROVIDES A SIMPLE MECHANISM FOR REVERSING THE MOTOR'S DIRECTION.

```
PROCEDURE IN1=FWDEND(VIN,IM,TL)
IF (VIN.LT.C.0) GO TC 10
IN1 = IM - TL
GC TC 15
10 IN1 = IM + TL
15 CONTINUE
ENDPROCEDURE
```

* THIS PROCEDURE RESETS THE VARIABLE THRST TO 0 AFTER EVERY 360 DEGREES OF MECHANICAL ROTATION. THIS IS FUNDAMENTAL TO THE SIMULATION OF ALL SWITCHING AND POSITION SENSING ACTION.

```
PROCEDURE THRST=RESET(JFAC,THDEG)
IS = JFAC * 360.0
THRST = THCEG - IS
IF (THRST.LT.360.0) GC TC 40
```

```

JFAC = JFAC + 1.0
40 CONTINUE
ENDPROCEDURE

```

```

** THIS PROCEDURE SERVES SEVERAL PURPOSES: FIRST, IT PROVIDES THE MODEL A
** MEANS OF APPLYING THE PROPER VOLTAGE TO THE APPROPRIATE WINDINGS WHICH
** SIMULATES GENERAL COMMUTATION. SECONDS, IT SETS THE VARIABLES SEL THRU
** SEL3 AND SW1 THRU SW6 TO LOGIC LEVELS 1 OR 0. THIS SIMULATES THE ACTION
** OF HALL EFFECT SENSORS BEING TURNED ON OR OFF IN THE FORMER CASE AND
** SIMULATES FETTER TRANSISTORS BEING ENERGIZED OR SWITCHED OFF IN THE
** LATTER CASE. THCON IS THE VARIABLE THROUGH WHICH THE SWITCHING LOGIC
** IS IMPLEMENTED.

```

```

PROCEDURE VA,VB,VC,SEL,SE2,SE3,SW1,SW2,SW3,SW4,SW5,SW6=VOLT(THCON,VIN2)
IF (THCCN .GE.180.) GC TC 45
GO TO 46

```

```

45 THCCN = THCCN - 180.
46 CONTINUE

```

```

IF (THCCN .GE. 0. .AND. THCON .LT. 30.) GO TC 50
IF (THCCN .GE. 30. .AND. THCCN .LT. 60.) GO TC 51
IF (THCCN .GE. 60. .AND. THCCN .LT. 90.) GO TC 52
IF (THCCN .GE. 90. .AND. THCCN .LT. 120.) GO TC 53
IF (THCCN .GE. 120. .AND. THCCN .LT. 150.) GO TC 54
IF (THCCN .GE. 150. .AND. THCON .LT. 180.) GO TC 55

```

```

50 VA = 0.

```

```

VB = VIN2

```

```

VC = VIN2

```

```

SE1 = 1.

```

```

SE2 = 1.

```

```

SE3 = 1.

```

```

SW1 = 1.

```

```

SW2 = 1.

```

```

SW3 = 1.

```

```

SW4 = 1.

```

```

SW5 = 1.

```

```

SW6 = 1.

```

```

TC = 60.

```

```

VA = 0.

```

```

VB = 0.

```

```

VC = 1.

```

```

SE1 = 1.

```

```

SE2 = 1.

```

```

SE3 = 1.

```

```

SW1 = 1.

```

```

SW2 = 1.

```

```

SW3 = 1.

```

```

51

```



```

SE3 = 1.
SW1 = 0.
SW2 = 1.
SW3 = 0.
SW4 = 0.
SW5 = 1.
SW6 = 0.
GC TCINUE
60 CONTINUE
ENDPFCCCLURE

TERMINAL BASIC CC MOTOR SYSTEM
TIMER FINTIM = .040, QUIDEL = .0004, PRCEL = .0004
TIMER THRTIME, IMA, IMB, IMC, IMT, IM, WM, WMRPM
PRINT SE1, SE2, SE3, SW1, SW2, SW3, SW4, SW5, SW6
LABEL MCTCF SPEED DUE TO STEP INPUT
PAGE MERGE

* PAGE XYPLCT
ENC
STCP

ENDJCB
/*

```


C. REVISION TWO

In the following program, the motor's air gap flux is treated as the average value of the sum of the flux acting in two windings as explained in Chapter Five. For convenience of study, both windings are again lumped into a single winding as in the prototype. This facilitates a closer focussing on the effects of variable flux on motor behavior.

```

//THCCSMP2 JCE (2672,0116), 'THOMAS-LAB6', CLASS=C
//*MAIN CRG=NF GVM1.2672P
// EXEC CSMPX\
//X. CCMPRINT CC DUMMY
//X. SYSPRINT CC DUMMY
//X. SYSIN DC *

* VERSION THREE - THIS PURPOSE OF THIS PROGRAM IS TO TREAT THE AIR GAP
* FLUX AS THE AVERAGE VALUE OF THE SUM OF THE FLUX ACTING IN TWO
* WINDINGS AS EXPLAINED IN CHAPTER FIVE. FOR CONVENIENCE OF STUDY, BCTH
* WINDINGS ARE LUMPED INTO ONE WINDING AS IN VERSION ONE IN ORDER TO
* FACILITATE CLOSE STUDY OF THE EFFECTS OF VARIABLE FLUX ON MOTOR
* BEHAVIOR.

INITIAL
CONSTANT KT = 15.5, BM = 0.00015, BL = 0.0, JL = 0.0, N = 1.0, ...
JM = 0.001, KB = 0.112, PI = 3.14159265, PHIAVG = 1.631, KK1 = 1.631
PARAMETER LA = .0016, RA = 2.740, ...
TL = (0.0, 32.0, 64.0, 96.0, 128.0)

* KT -- TORQUE CONSTANT (CZ-IN/AMP)
* KB -- BACK EMF CONSTANT (VOLT/RAD/S)
* JM -- RESISTANCE OF THE MOTOR (OHM)
* BM -- VISCOUS FRICTION COEFFICIENT OF THE MOTOR (OZ-IN/RAD/S)
* BL -- VISCOUS FRICTION COEFFICIENT OF THE LOAD
* BLF -- VISCOUS FRICTION COEFFICIENT OF LOAD THRU REDUCTION GEARS
* JB -- TOTAL VISCOUS FRICTION COEFFICIENT OF THE MOTOR SYSTEM
* JM -- INERTIA OF THE MOTOR
* JLF -- INERTIA OF THE LOAD THRU REDUCTION GEARS
* JL -- INERTIA OF THE LOAD
* J -- TOTAL INERTIA OF THE MOTOR SYSTEM
* TL -- TORQUE
* LA -- LA/RA -- THE ELECTRICAL TIME CONSTANT OF THE MOTOR
* A1 = J/E -- THE MECHANICAL TIME CONSTANT OF THE MOTOR
* KBP -- THE NORMALIZED PRODUCT OF KB AND PHIAVG
* KTF -- THE NORMALIZED PRODUCT OF KT AND PHIAVG
* PHIAVG -- THE AVERAGE VALUE OF SINUSOIDALLY VARYING FLUX

NOSORT
BLF = BL/(N**2)
JLF = JL/(N**2)
J = JM + JLF
B = BM + BLF
A1 = LA / RA

```

```

A2 = J / B
THRST = 0.0
JFAC = 0.0
KTF = KT * FFI AVG * (1/KK1)
KBF = KE * FFI AVG * (1/KK1)

```

```

DYNAMIC
VIF= 30.0 * STEP(0.0)
VIE = 0.0
VIN = VIF + VIB
VIN1 = VIN - VEMF
VIN2 = VIN1 * (1.0/RA)
IMF = REALPL(0.0,A1,VIN2)
TM = KTF * IMP
TN2 = TN1 * (1.0/C/B)
WM = REALPL(0.0,A2,TN2)
WMRPM = WM * (30./PI)
WMPMR = WMRPM/N
THETA = INTGR(0.0,WM)
THCEG = THETA * (180.0/PI)
THCCN = THRST
PWR = WM * TM * .0070615
VEMF = KBP * WM

```

* THIS PROCEDURE PROVIDES A SIMPLE MECHANISM FOR REVERSING THE MOTOR'S DIRECTION.

```

PROCEDURE TN1=FWDWD(VIN,TM,TL)
IF (VIN.LT.0.0) GO TC 10
TN1 = TM - TL
GO TC 15
10 TN1 = TM + TL
15 CONTINUE
ENDPROCEDURE

```

* THIS PROCEDURE RESETS THE VARIABLE THRST TO 0 AFTER EVERY 360 DEGREES OF MECHANICAL ROTATION. THIS IS FUNDAMENTAL TO THE SIMULATION OF ALL SWITCHING AND POSITION SENSING ACTION.

```

PROCEDURE THRST=RESET(JFAC,TDEG)
TS = JFAC * 360.0
THRST = TDEG - TS
IF (THRST.LT.360.) GO TO 40

```

```

JFAC = JFAC + 1.0
40 CONTINUE
ENDPROCEDURE

* THE PURPOSE OF THIS PROCEDURE IS TO SET THE VARIABLES SEL THRU
  SE3 AND SW1 THRU SW6 TO LOGIC LEVELS 1 OR 0. THIS SIMULATES THE ACTION
  OF HALL EFFECT SENSORS BEING TURNED ON OR OFF IN THE FORMER CASE AND
  SIMULATES POWER TRANSISTORS BEING ENERGIZED OR SWITCHED OFF IN THE
  LATTER CASE. THCON IS THE VARIABLE THROUGH WHICH THE SWITCHING LOGIC
  IS IMPLEMENTED.

PROCEDURE SEL,SE2,SE3,SW1,SW2,SW3,SW4,SW5,SW6=VOLT(THCON)
  IF (THCCN .GE.180.) GO TO 45
  GO TO 46
  THCON = THCCN - 180.
45 CONTINUE
  IF (THCCN .GE. 0.) AND .LT. 30.) GO TO 50
  IF (THCCN .GE. 30.) AND .LT. 60.) GO TO 51
  IF (THCCN .GE. 60.) AND .LT. 90.) GO TO 52
  IF (THCCN .GE. 90.) AND .LT. 120.) GO TO 53
  IF (THCCN .GE. 120.) AND .LT. 150.) GO TO 54
  IF (THCCN .GE. 150.) AND .LT. 180.) GO TO 55
  SEL = 1.
  SE2 = 1.
  SE3 = 1.
  SW1 = 0.
  SW2 = 0.
  SW3 = 0.
  SW4 = 0.
  SW5 = 0.
  SW6 = 0.
  TC = 1.
  GO TO 51
1
2
3
4
5
6
7
8
9
10
11
12
13
14
15
16
17
18
19
20
21
22
23
24
25
26
27
28
29
30
31
32
33
34
35
36
37
38
39
40
41
42
43
44
45
46
47
48
49
50
51
52
53
54
55
56
57
58
59
60
61
62
63
64
65
66
67
68
69
70
71
72
73
74
75
76
77
78
79
80
81
82
83
84
85
86
87
88
89
90
91
92
93
94
95
96
97
98
99
100
101
102
103
104
105
106
107
108
109
110
111
112
113
114
115
116
117
118
119
120
121
122
123
124
125
126
127
128
129
130
131
132
133
134
135
136
137
138
139
140
141
142
143
144
145
146
147
148
149
150
151
152
153
154
155
156
157
158
159
160
161
162
163
164
165
166
167
168
169
170
171
172
173
174
175
176
177
178
179
180
181
182
183
184
185
186
187
188
189
190
191
192
193
194
195
196
197
198
199
200
201
202
203
204
205
206
207
208
209
210
211
212
213
214
215
216
217
218
219
220
221
222
223
224
225
226
227
228
229
230
231
232
233
234
235
236
237
238
239
240
241
242
243
244
245
246
247
248
249
250
251
252
253
254
255
256
257
258
259
260
261
262
263
264
265
266
267
268
269
270
271
272
273
274
275
276
277
278
279
280
281
282
283
284
285
286
287
288
289
290
291
292
293
294
295
296
297
298
299
300
301
302
303
304
305
306
307
308
309
310
311
312
313
314
315
316
317
318
319
320
321
322
323
324
325
326
327
328
329
330
331
332
333
334
335
336
337
338
339
340
341
342
343
344
345
346
347
348
349
350
351
352
353
354
355
356
357
358
359
360
361
362
363
364
365
366
367
368
369
370
371
372
373
374
375
376
377
378
379
380
381
382
383
384
385
386
387
388
389
390
391
392
393
394
395
396
397
398
399
400
401
402
403
404
405
406
407
408
409
410
411
412
413
414
415
416
417
418
419
420
421
422
423
424
425
426
427
428
429
430
431
432
433
434
435
436
437
438
439
440
441
442
443
444
445
446
447
448
449
450
451
452
453
454
455
456
457
458
459
460
461
462
463
464
465
466
467
468
469
470
471
472
473
474
475
476
477
478
479
480
481
482
483
484
485
486
487
488
489
490
491
492
493
494
495
496
497
498
499
500
501
502
503
504
505
506
507
508
509
510
511
512
513
514
515
516
517
518
519
520
521
522
523
524
525
526
527
528
529
530
531
532
533
534
535
536
537
538
539
540
541
542
543
544
545
546
547
548
549
550
551
552
553
554
555
556
557
558
559
560
561
562
563
564
565
566
567
568
569
570
571
572
573
574
575
576
577
578
579
580
581
582
583
584
585
586
587
588
589
590
591
592
593
594
595
596
597
598
599
600
601
602
603
604
605
606
607
608
609
610
611
612
613
614
615
616
617
618
619
620
621
622
623
624
625
626
627
628
629
630
631
632
633
634
635
636
637
638
639
640
641
642
643
644
645
646
647
648
649
650
651
652
653
654
655
656
657
658
659
660
661
662
663
664
665
666
667
668
669
670
671
672
673
674
675
676
677
678
679
680
681
682
683
684
685
686
687
688
689
690
691
692
693
694
695
696
697
698
699
700
701
702
703
704
705
706
707
708
709
710
711
712
713
714
715
716
717
718
719
720
721
722
723
724
725
726
727
728
729
730
731
732
733
734
735
736
737
738
739
740
741
742
743
744
745
746
747
748
749
750
751
752
753
754
755
756
757
758
759
760
761
762
763
764
765
766
767
768
769
770
771
772
773
774
775
776
777
778
779
780
781
782
783
784
785
786
787
788
789
790
791
792
793
794
795
796
797
798
799
800
801
802
803
804
805
806
807
808
809
810
811
812
813
814
815
816
817
818
819
820
821
822
823
824
825
826
827
828
829
830
831
832
833
834
835
836
837
838
839
840
841
842
843
844
845
846
847
848
849
850
851
852
853
854
855
856
857
858
859
860
861
862
863
864
865
866
867
868
869
870
871
872
873
874
875
876
877
878
879
880
881
882
883
884
885
886
887
888
889
890
891
892
893
894
895
896
897
898
899
900
901
902
903
904
905
906
907
908
909
910
911
912
913
914
915
916
917
918
919
920
921
922
923
924
925
926
927
928
929
930
931
932
933
934
935
```

```

000010
== == TC
23456
SWWWE
53
123123456
SWWWE
54
123123456
SWWWE
60
TC INUE
ENDPFCCEURE

```

```

TERMINAL BASIC CC MOTOR SYSTEM
TITLE FINIM = .040, OUTDEL = .0004, PRCEL = .0004
TIMER IFRST, VEMF, IMP, TM, WM, WMRPM, PWR
PAGE ENL
STCP
ENDJCB
/*

```

D. REVISION THREE

The purpose of this version of the program is treat the air gap flux as varying in simple sinusoidal fashion. The total system flux is treated as the algebraic sum of the flux developed in the two active windings.

```

//THCCSMF2 JCE (2672,0116), 'THOMAS-LAB6', CLASS=C
//*MAIN CRG=NFGVM1.2672P
//EXEC CSMPL
//X.COMPRINT CC DUMMY
//X.SYSPRINT LL DUMMY
//X.SYSIN DC *

```

* VERSION FOUR -- THE PURPOSE OF THIS VERSION OF THE PROGRAM IS TO
 * TREAT THE AIR GAP FLUX AS VARYING IN SINUSOIDAL FASHION. THE TOTAL
 * SYSTEM FLUX IS TREATED AS THE ALGEBRAIC SUM OF THE FLUX DEVELOPED IN
 * THE TWO ACTIVE WINDINGS AS EXPLAINED IN CHAPTER FIVE.

```

INITIAL
CONSTANT KT = 15.4, KE = 0.1089, PI = 3.14159265, BL = 0.0, JL = 0.0, N = 1.0, ...
JM = 0.001, LA = .0016, RA = 2.700, ...
PARAMETER LA = .0016, RA = 2.700, ...
KK2 = 1.6551, TL = (0.0, 32.0, 64.0, 96.0, 128.0)

```

```

* KT -- TORQUE CONSTANT (CZ-IN/AMP)
* KB -- BACK EMF CONSTANT (VCLT/RAD/S)
* RA -- RESISTANCE OF THE MOTOR (OHM)
* BM -- VISCOUS FRICTION COEFFICIENT OF THE MOTOR (OZ-IN/RAD/S)
* BL -- VISCOUS FRICTION COEFFICIENT OF THE LCAD
* BLF -- VISCOUS FRICTION COEFFICIENT OF LCAD THRU REDUCTION GEARS
* B -- VISCOUS FRICTION COEFFICIENT OF THE MOTOR SYSTEM
* JM -- TCTAL VISCOUS FRICTION OF THE MOTOR (OZ-IN/S-S)
* JL -- INERTIA OF THE MOTOR
* JLF -- INERTIA OF THE LCAD THRU REDUCTION GEARS
* J -- TCTAL INERTIA OF THE MOTOR SYSTEM
* TL -- TCTAL TORQUE (CZ-IN)
* A1 = LA/RA -- ELECTRICAL TIME CONSTANT OF THE MOTOR
* A2 = J/E -- THE MECHANICAL TIME CONSTANT OF THE MOTOR
* JFAC -- A COUNTER VARIABLE
* KBFP -- THE NORMALIZED PRODUCT OF KB AND THE COMPOSITE VARIABLE FLUX
* KTFP -- THE NORMALIZED PRODUCT OF KT AND THE COMPOSITE VARIABLE FLUX

```

```

NOSOF = EL/(N**2)
BLF = JL/(N**2)
J = JM + JLF
B = BM + BLF
A1 = LA / RA
A2 = J / B
THRST = 0.0

```


JFAC = C.O

```

DYNAMIC 3 C.O * STEP(0.0)
VIF= C.O
VIB = VIF + VIB
VIN = VIN - VEMF
VIN1 = VIN * (1.0/RA)
IMF = REALFL(0.0,A1,VIN2)
TM = K TTP * IMP
TN2 = TN1 * (1.0/B)
WMRPM = REALPL(C.O,A2,TN2)
WMFPM/N = WMFPM/N
BEMFA = SIN(2.*THETA + (1 * PI/6))
BEMFB = SIN(2.*THETA + (9 * PI/6))
BEMFC = SIN(2.*THETA + (5 * PI/6))
THETA = INTGRL(C.O,WM)
THCCN = THETA * (180.0/PI)
PWR = WM * TM * .0070615
VEMF = KBPF * WM
KBFP = KB * EEMFT * (1/KK2)
KTTP = KT * EEMFT * (1/KK2)

```

* THIS PROCEDURE PROVIDES A SIMPLE MECHANISM FOR REVERSING THE MOTOR'S
* DIRECTION.

```

PROCEDURE TN1=FWDWD(VIN,TM,TL)
IF (VIN.LT.0.0) GO TG 10
TN1=TM-TL
GC TC 15
10 TN1=TM+TL
15 CONTINUE
ENDPROCEDURE

```

* THIS PROCEDURE RESETS THE VARIABLE THRST TO 0 AFTER EVERY 360 DEGREES
* OF MECHANICAL ROTATION. THIS IS FUNDAMENTAL TO THE SIMULATION OF ALL
* SWITCHING AND POSITION SENSING ACTION.

```

PROCEDURE THRST=RESET(JFAC,THDEG)
TS = JFAC * 360.0
THRST = THDEG - TS

```

```

IF (TFRST.LT.360.) GO TO 40
FAC = JFAC + 1.0
40 CONTINUE
ENDPROCEDURE

```

```

* THE PURPOSE OF THIS PROCEDURE IS TO SET THE VARIABLES SE1 THRU
* SE3 AND SW1 THRU SW6 TO LOGIC LEVELS 1 OR 0. THIS SIMULATES THE ACTION
* OF HALL EFFECT SENSORS BEING TURNED ON OR OFF IN THE FORMER CASE AND
* SIMULATES POWER TRANSISTORS BEING ENERGIZED OR SWITCHED OFF IN THE
* LATTER CASE. THCON IS THE VARIABLE THROUGH WHICH THE SWITCHING LOGIC
* IS IMPLEMENTED.

```

```

PROCEDURE SE1, SE2, SE3, SW1, SW2, SW3, SW4, SW5, SW6 = VOL1(THCON)
IF (THCCN .GE. 180.) GC TC 45
GO TO 46

```

```

45 THCON = THCCN - 180.
46 CONTINUE
IF (THCCN .GE. 0.) AND. THCCN .LT. 30.) GO TC 50
IF (THCCN .GE. 30.) AND. THCCN .LT. 60.) GO TC 51
IF (THCCN .GE. 60.) AND. THCCN .LT. 90.) GO TC 52
IF (THCCN .GE. 90.) AND. THCCN .LT. 120.) GO TC 53
IF (THCCN .GE. 120.) AND. THCCN .LT. 150.) GO TC 54
IF (THCCN .GE. 150.) AND. THCCN .LT. 180.) GO TC 55

```

```

50 SE1 = 1.
SE2 = 0.
SE3 = 0.
SW1 = 0.
SW2 = 0.
SW3 = 0.
SW4 = 1.
SW5 = 1.
SW6 = 0.
GC TC 60
51 SE1 = 1.
SE2 = 0.
SE3 = 1.
SW1 = 0.
SW2 = 0.
SW3 = 1.
SW4 = 1.
SW5 = 1.
SW6 = 0.
GC TC 60
52 SE1 = 1.
SE2 = 1.
SE3 = 1.
SW1 = 1.
SW2 = 1.
SW3 = 1.
SW4 = 1.
SW5 = 1.
SW6 = 0.
GC TC 60

```

```

1.0.0.0.0.1.60
= = = = =
SW1SW2SW3SW4SW5SW6TC
53 1.0.0.0.0.1.60
= = = = =
SW1SW2SW3SW4SW5SW6TC
54 1.0.0.0.0.1.60
= = = = =
SW1SW2SW3SW4SW5SW6TC
55 1.0.0.0.0.1.60
= = = = =
SW1SW2SW3SW4SW5SW6TC
60 CONTINUE
ENDPROCEDURE

```

* THE FOLLOWING PROCEDURE HAS THE SAME FORM AND EFFECT AS THE
 * PREVIOUS. IT IS USED HERE TO DETERMINE THE ALGEBRAIC SUM OF
 * THE VARIABLE FLUX COMPONENTS FOR USE IN COMPUTING THE MOTOR'S
 * APPROXIMATE BACK EMF (BEMF). THIS FUNCTION COULD AS EASILY
 * HAVE BEEN CALCULATED IN THE PREVIOUS PROCEDURE EXCEPT THAT
 * THERE WAS INSUFFICIENT ROOM TO ACCOMMODATE THE ADDITIONAL VARIABLES.

```

PROCEDURE BEMFT=V(LT (THCCN, BEMFA, BEMFB, BEMFC)
IF (THCCN .GE.180.) GC TC 65
GC TC 66
65 THCCN = THCCN - 180.
66 CONTINUE
IF (THCCN .GE. 0. AND. THCCN .LT. 30.) GO TC 70
IF (THCCN .GE. 30. AND. THCCN .LT. 60.) GO TC 71
IF (THCCN .GE. 60. AND. THCCN .LT. 90.) GO TC 72
IF (THCCN .GE. 90. AND. THCCN .LT. 120.) GO TC 73
IF (THCCN .GE. 120. AND. THCCN .LT. 150.) GO TC 74
IF (THCCN .GE. 150. AND. THCCN .LT. 180.) GO TC 75
70 BEMFT = BEMFA - BEMFB
71 GO TC 80
71 BEMFT = BEMFA - BEMFC
72 GO TC 80
72 BEMFT = BEMFB - BEMFC
73 GO TC 80
73 BEMFT = BEMFB - BEMFA
74 GO TC 80
74 BEMFT = BEMFC - BEMFA
75 GO TC 80
75 BEMFT = BEMFC - BEMFB
80 CONTINUE
ENDPROCEDURE

```

```

TERMINAL BASIC CC NOTCR SYSTEM = .0004, PRCEL = .0004
TITLE FIN IN = .040, OLIDEL = .0004, PRCEL = .0004
TIMER FIN IN = .040, OLIDEL = .0004, PRCEL = .0004
* PRINT SE1, SE2, SE3, SW1, SW2, SW3, SW4, SW5, SW6
PRINT THRST, BEMFT1, BEMFT, VEMF, IMP, IM, WN, WMRFM, PWR
PAGE MERGE
ENC STCP
ENDJCB
/*

```

E. REVISION FOUR

This version of the model treats the flux as varying according to the sum of a sinusoid of fundamental frequency and its fifth harmonic as explained in Chapter Five. The total flux is again approximated as the algebraic sum of the flux developed in two windings at a time.

 VERSION FIVE -- THE PURPOSE OF THIS VERSION OF THE PROGRAM IS TO
 TREAT THE FLUX AS VARYING ACCORDING TO THE SUM CF A SINUSOID OF
 FUNDAMENTAL FREQUENCY AND ITS FIFTH HARMONIC AS EXPLAINED IN CHAPTER
 FIVE. THE TOTAL FLUX IS APPROXIMATED AS THE ALGEBRAIC SUM CF THE FLUX
 DEVELOPED IN TWO WINDINGS AT A TIME.

```

** ** ** ** ** ** ** ** ** ** **  TCRQLE CCNSTANT (CZ-IN/AMP)
** ** **  --  BACK EMF CCNSTANT (VCLT/RAD/S)
** ** **  --  RESISTANCE OF THE MCTCR (OHM)
** ** **  --  VISCCLSS FRICTCN COEFFICIENT CF THE MCTOR (OZ-IN/RAD/S)
** ** **  --  VISCCLSS FRICTCN COEFFICIENT CF THE LCAD THRL REDUCTION GEARS
** ** **  --  VISCCLSS FRICTCN COEFFICIENT OF LCAD THRL REDUCTION GEARS
** ** **  --  VISCCLSS FRICTCN COEFFICIENT OF THE MCTOR SYSTEM
** ** **  --  TOTAL VISCUS FRICTCN OF THE MCTOR (OZ-IN/S-S)
** ** **  --  INERTIA CF THE LCAD
** ** **  --  INERTIA CF THE LCAD THRL REDUCTION GEARS
** ** **  --  INERTIA CF THE LCAD THRL REDUCTION GEARS
** ** **  --  TCTAL INERTIA OF THE MCTOR SYSTEM
** ** **  --  TCTAL INERTIA (CZ-IN)
** ** **  --  LA/RD TCRQLE (CZ-IN)
** ** **  --  LA/RD -- THE INVERSE ELECTRICAL TIME CCNSTANT
** ** **  --  J/B -- THE INVERSE MECHANICAL TIME CCNSTANT
** ** **  --  JFAC = COUNTER VARIABLE
** ** **  --  JFAC = A COUNTER VARIABLE
** ** **  --  JFACPP -- THE NORMALIZED PRCDCT OF KB AND THE CCMPCSITE VARIABLE
** ** **  --  KTFPP -- THE NORMALIZED PRCDCT OF KT AND THE CCMPCSITE VARIABLE

```

70

```

A2 = J / B
THRST = 0.0
JFAC = 0.0

DYNAMIC
VIF = 30.0 * STEP(0.0)
VIE = 0.0
VIN = VIF + VIB
VIN1 = VIN - VEMF
VIN2 = VIN1 * (1.0/RA)
IMF = REALPL(0.0,A1,VIN2)
TM = KTPPP * IMF
TN2 = TN1 * (1.0/B)
WM = REALPL(C.0,A2,TN2)
WMFPM = WM * (30.0/PI)
WMRPMR = WMFPM/N
BEMFA = (3.0 * SIN(2.0 * THETA + (1*PI/6)) + .59 * SIN(10.0 * THETA + (5*PI/6)))
BEMFB = (3.0 * SIN(2.0 * THETA + (9*PI/6)) + .59 * SIN(10.0 * THETA + (9*PI/6)))
BEMFC = (3.0 * SIN(2.0 * THETA + (5*PI/6)) + .59 * SIN(10.0 * THETA + (1*PI/6)))
THCEG = INTCRL(C.0,WM)
THCON = THCEG * THRT
PWR = WM * TM * .0706155
VEMF = KBPFF * BEMF * (1/KK2)
KBPPP = KB
KTPPP = KT * BEMF * (1/KK3)

```

* THIS PROCEDURE PROVIDES A SIMPLE MECHANISM FOR REVERSING THE MOTOR'S
* DIRECTION.

```

PROCEDURE TN1=FWDEND(VIN,TM,TL)
IF(VIN.LT.C.0) GO TO 1C
TN1 = TM - TL
GO TO 15
10 TN1 = TM + TL
15 CONTINUE
ENDPROCEDURE

```

* THIS PROCEDURE RESETS THE VARIABLE THRST TO 0 AFTER EVERY 300 DEGREES
* OF MECHANICAL ROTATION. THIS IS FUNDAMENTAL TO THE SIMULATION OF ALL
* SWITCHING AND POSITION SENSING ACTION.

```

PROCEDURE THRST=RESET(JFAC,THDEG)

```


* COULD NOT ACCUMDATE THE ADDITIONAL VARIABLES.

```

PROCEDURE BEMFT=VCLT (THCCN,BEMFA,BEMFB,BEMFC)
  IF (THCCN .GE.180.) GC TC 65
  GO TO 66
65 THCCN = THCCN - 180.
66 CONTINUE
  GE. 0. AND. THCCN .LT. 30.) GC TC 70
  IF (THCCN .GE. 30. AND. THCCN .LT. 60.) GC TC 71
  IF (THCCN .GE. 60. AND. THCCN .LT. 90.) GC TC 72
  IF (THCCN .GE. 90. AND. THCCN .LT. 120.) GC TC 73
  IF (THCCN .GE. 120. AND. THCCN .LT. 150.) GC TC 74
  IF (THCCN .GE. 150. AND. THCCN .LT. 180.) GC TC 75
70 BEMFT = BEMFA - BEMFB
  GC TC 80
71 BEMFT = BEMFA - BEMFC
  GC TC 80
72 BEMFT = BEMFB - BEMFC
  GC TC 80
73 BEMFT = BEMFB - BEMFA
  GC TC 80
74 BEMFT = BEMFC - BEMFA
  GC TC 80
75 BEMFT = BEMFC - BEMFB
  GC TC 80
80 CONTINUE
ENDPROCEDURE

```

```

TERMINAL BASIC CC MOTOR SYSTEM
TITLE FINISH=.028, OUTDEL = .0004, PRCEL = .0C04
** PRINT THRST, SE1, SE2, SE3
** PRINT SW1, SW2, SW3
** PRINT VEMF, SW4, SW5, SW6
  LABEL MCTCF, IMP, TM, WMRPM, PWR
  PAGE MERGE
  ENC
  STOP
ENDJCB
/*

```

APPENDIX B

SAMPLE OUTPUT

The following is a sample of the type of information the model can provide. In this particular case, the fourth revision of the basic prototype, the harmonic flux case, was used. For completeness, the motor was run at loads from 0.0 up through 96.0 oz-in, which was the range of loads with which all analysis was performed. In addition to such motor variables as speed, current and power, a sampling of the feedback from Hall effect sensors as well as the switching action of the power transistors is included.

1	840000	-000000	24.208	1.2318	16.099	2505.3	29.826
1	880000	-000000	27.358	1.4412	21.046	2534.2	39.436
1	920000	-000000	31.461	1.77432	12.885	2557.2	24.366
1	960000	-000000	35.751	1.6032	2.5535	2537.1	4.887
2	000000	-000000	25.264	1.500325	16.584	2506.1	12.737
2	040000	-000000	27.625	1.2665	10.978	2506.5	39.339
2	080000	-000000	31.571	1.7237	20.116	2557.3	22.513
2	120000	-000000	30.016	1.5259	2.4436	2535.2	4.581

1 BAL TIME = 2.8000 E-02

1	200000	-000000	25.545	IMP 54200	TM 7.4754	WMRPM 2505.2	PWR 13.848
2	240000	-000000	25.337	1.2991	17.055	2507.8	31.622
2	280000	-000000	27.895	1.4032	20.862	2537.3	39.151
2	320000	-000000	31.660	1.67730	21.348	2535.2	21.448
2	360000	-000000	29.776	1.4855	13.618	2504.5	4.433
2	400000	-000000	25.350	1.58499	17.096	2508.7	14.480
2	440000	-000000	24.426	1.3294	17.509	2539.0	32.570
2	480000	-000000	28.167	1.3797	20.567	2557.2	19.373
2	520000	-000000	31.728	1.62964	10.567	2531.6	14.582
2	560000	-000000	29.525	1.4809	17.944	2503.8	15.834
2	600000	-000000	25.168	1.62899	20.552	2509.1	33.304
2	640000	-000000	28.532	1.3573	17.948	2541.6	18.493
2	680000	-000000	24.474	1.3532	10.481	2529.1	38.523
2	720000	-000000	31.774	1.58284	20.797	2559.5	14.158
2	760000	-000000	29.274	1.5081	20.361	2529.5	16.848
2	800000	-000000	24.998	1.67380	9.1025	2502.9	

1 BAL TIME = 2.8000 E-02

1	000000	-000000	0.000	IMP 0	TM 0.089	WMRPM 0	PWR 0
1	040000	-000000	9.883	5.4719	9.21	73.949	5.0357
1	080000	-000000	20.323	7.6010	13.634	387.70	37.611
1	120000	-000000	4.553	8.1839	132.381	774.33	78.095
1	160000	-000000	13.585	7.5780	120.339	1132.1	101.976
2	200000	-000000	16.238	6.7204	120.595	1411.0	104.275
2	240000	-000000	16.890	6.0510	77.438	1609.3	98.777
2	280000	-000000	18.578	5.6101	70.835	1751.5	94.379
2	320000	-000000	22.542	5.1302	66.055	1869.7	97.652
2	360000	-000000	25.452	4.2843	55.135	2053.6	83.608
2	400000	-000000	24.892	3.2359	46.585	2076.1	55.150
2	440000	-000000	21.927	2.5434	36.937	2061.0	60.782
2	480000	-000000	19.847	3.0453	46.215	2047.0	50.453
2	520000	-000000	20.514	3.4185	45.235	2052.2	70.142
2	560000	-000000	23.443	3.234	45.235	2077.7	75.133

[illegible]

[illegible]

1550 1582 1614 1593 1564 1534 1552 1584 1613 1592 1569 1535 1553 1586 1612 1590

[illegible][illegible]

16. 6452
18. 6620
20. 5082
17. 7666
15. 8577
14. 8246
16. 7767
18. 5031
20. 6415
17. 7657
15. 8577
14. 8589
16. 7879
18. 8855
20. 9414
17. 5517

[illegible]

P_{WR} 73. 76. 83. 90. 94. 89. 80. 75. 77. 83. 91. 94. 88. 80. 74.

W MRPM 1561.1 1539.0 1535.7 1558.9 1612.4 1588.6 1559.2 1536.4 1537.5 1590.9 1614.1 1587.1

TM 6 4.0378
6 4.5322
7 3.0698
7 3.0986
8 0.9566
7 7.775
6 3.8978
6 4.1641
7 3.8688
7 3.2951
7 4.5169
6 3.805

IMP 4.7155
5.1770
5.3333
5.45016
4.5539
4.4539
4.1803
4.3156
5.7446
5.20024
5.23840
5.3340
5.5235
4.42778
4.1768
4.3354

15. 844
14. 356
15. 995
18. 074
20. 323
19. 352
17. 592
14. 836
15. 429
17. 119
19. 100
20. 082
19. 227
17. 268

[illegible]

00

PAR
-11.603
-5.1202
23.353

WMPM
0
-161.51
-47.044
190.70

TM 0
97.146
147.188
165.88

IMP 0 7742
5. 7552
8. 8620

-2.0090
 -2.58469
 -2.3713

TIME
4.00000D-04
8.00000D-04
1.20000D-03

30

[illegible]

00	TIME	=	THRST	SE1	SE2	SE3
0	4	000000	0	1	0	1
1	8	000000	16264	1	0	1
1	1	000000	10994	1	0	1
2	2	000000	15266	1	0	1
2	2	000000	10664	1	0	1
3	3	000000	19702	1	0	1
3	3	000000	25217	1	0	1
4	4	000000	37045	1	0	1
4	4	000000	43062	1	0	1
5	5	000000	49125	1	0	1
6	6	000000	55273	1	0	1
6	6	000000	61471	1	0	1
7	7	000000	67677	1	0	1
7	7	000000	73738	1	0	1
8	8	000000	79860	1	0	1
8	8	000000	85011	1	0	1
9	9	000000	91158	1	0	1
9	9	000000	104125	1	0	1
1	1	000000	116238	1	0	1
1	1	000000	128446	1	0	1
1	1	000000	134465	1	0	1
1	1	000000	140555	1	0	1
1	1	000000	146728	1	0	1
1	1	000000	15275	1	0	1
1	1	000000	15883	1	0	1
1	1	000000	164906	1	0	1
1	1	000000	170913	1	0	1
1	1	000000	176027	1	0	1
1	1	000000	18345	1	0	1
1	1	000000	18951	1	0	1
1	1	000000	19512	1	0	1
1	1	000000	20139	1	0	1
1	1	000000	20745	1	0	1
1	1	000000	21351	1	0	1
1	1	000000	21957	1	0	1
1	1	000000	22561	1	0	1
1	1	000000	23173	1	0	1
1	1	000000	23749	1	0	1
1	1	000000	24375	1	0	1

LIST OF REFERENCES

1. Fiscal Year 1983 NAVAIR Strike Warfare Technology Plan, Advanced Missile Control Devices, by R. F. Dettling, September 1982.
2. Speckhart, F. H. and Green, A. L., A Guide to Using CSMP - The Continuous System Modeling Program, Prentice-Hall, Inc., 1976.
3. Kuo, B. C., Automatic Control Systems, 4th ed., Prentice-Hall, Inc., 1982.
4. Fitzgerald, A. E. and Kingsley, Jr., Charles, Electric Machinery, McGraw-Hill Book Company, Inc., 1952.
5. D.C. Motors, Speed Controls, Servo Systems, An Engineering Handbook, 4th ed., Electrocraft Corporation, 1978.

BIBLIOGRAPHY

Demerdash, N.A., Miller, R.H., Nehl, T.W., "Comparison Between Features and Performance Characteristics of Fifteen HP Samarium Cobalt and Ferrite Based Brushless DC Motors Operated by the Same Power Conditioner," IEEE Transactions on Power System Apparatus and Systems, v. PAS-102, January 1983.

Demerdash, N.A. and Nehl, T.W., Dynamic Modeling of Brushless DC Motor-Power Conditioner Unit for Electromechanical Actuator Application, paper presented at IEEE Power Electronics Specialists Conference, San Diego, California, 9 June 1979.

Miller, T.J., "Rare Earth Magnets Contribute to Small Size, High Torque of New Motor Designs," Control Engineering, May, 1983.

Murugesan, S., "An Overview of Electric Motors for Space Applications," IEEE Transactions on Industrial Electronics and Control Instrumentation, v. IECI-28, November, 1981.

National Aeronautics and Space Administration Report cr-160349, Numerical Simulation of Dynamics of Brushless DC Motors for Aerospace and Other Applications, by N.A.O. Demerdash and T.W. Nehl, 15 November 1979.

National Aeronautics and Space Administration Report tm-80445, Analytical Modeling of the Dynamics of Brushless DC Motors for Aerospace Applications, A Conceptual Framework, by N.A.O. Demerdash, F.E. Eastman, and R.G. Chilton, 18 August, 1976.

Oppenheimer, M., "In IC Form, Hall-Effect Devices Can Take On Many New Applications," Electronics, August 2, 1971.

Society of Automotive Engineers, Inc. Technical Paper Series, #780581, Electromechanical Actuator Technology Program, by J.T. Edge, April 1978.

INITIAL DISTRIBUTION LIST

	No.	Copies
1. Defense Technical Information Center Cameron Station Alexandria, Virginia 22314	2	
2. Library, Code 0142 Naval Postgraduate School Monterey, California 93943	2	
3. Department Chairman, Code 62 Department of Electrical Engineering Naval Postgraduate School Monterey, California 93943	1	
4. Professor Alex Gerba, Jr., Code 62Gz Department of Electrical Engineering Naval Postgraduate School Monterey, California 93943	2	
5. Professor George J. Thaler, Code 62Tr Department of Electrical Engineering Monterey, California 93943	1	
6. Naval Weapons Center, China Lake Weapons Power Systems Branch Code 3275 Attn: R.F. Dettling China Lake, California 93555	2	
7. LT Steven M Thomas 998 Leahy Road Monterey, CA 93940	1	

210815

Thesis

T4262 Thomas

c.1 CSMP modeling of
brushless DC motors.

210815

Thesis

T4262 Thomas

c.1 CSMP modeling of
brushless DC motors.

CSMP modelling of brushless DC motors.



3 2768 001 01096 0

DUDLEY KNOX LIBRARY